Natural variation in the *FtNAC2* promoter regulates quercetin accumulation and drought tolerance in Tartary buckwheat

Jing Wang[1,2,3,6†], Wei Li[1,6†], Dongqing Fan[1,6†], Yuqi He[1,6], Yaliang Shi[1,6], Hao Lin[1,6], Marie-Laure Fauconnier[2], Giorgia Purcaro[3], Muriel Quinet[4], Manon Genva[2], Kaixuan Zhang[1,6], Mengqi Ding[5*] and Meiliang Zhou[1,6*]

[1]National Key Facility for Crop Gene Resources and Genetic Improvement Institute of Crop Sciences, Chinese Academy of Agricultural Sciences, Beijing 100081, China.

[2]The Laboratory of Chemistry of Natural Molecules, Gembloux Agro-Bio Tech, University of Liège, Passage des Déportés, 2 - 5030 Gembloux, Belgium.

[3]The Analytical Chemistry Lab, Chemistry for Sustainable Food and Environmental Systems, Gembloux Agro-Bio Tech, University of Liège, Bât. G1, Passage des Déportés 2, 5030 Gembloux, Belgium.

[4]Groupe de Recherche en Physiologie Végétale (GRPV) Earth and Life Institute-Agronomy (ELI-A) Université Catholique de Louvain Croix du Sud 45, boîte L7.07.13, Louvain-la-Neuve B-1348, Belgium.

[5]College of Agronomy and Biotechnology, Southwest University, Chongqing, 400715 China

[6]Sanya Nan Fan Research Institute, Chinese Academy of Agricultural Sciences, Sanya, 572024, Hainan, China.

***For correspondence (e-mail: dingmengqi@swu.edu.cn and zhoumeiliang@caas.cn).**

[†]These authors contributed equally to this work.

Abstract

Tartary buckwheat, valued for its nutritious and medicinal quercetin. Following two independent domestication events, distinct quercetin accumulation patterns have emerged between the southwestern (SL) and northern (NL) landrace populations. However, the genetic mechanisms underlying these metabolic divergences remain elusive. Here, we identified the transcription factor FtNAC2 through genome-wide association study (GWAS) of quercetin content in 480 accessions of Tartary buckwheat. Haplotype analysis identified two single nucleotide polymorphisms (SNPs) in the *FtNAC2* promoter that defined three major haplotypes, with higher promoter activity and gene expression observed in Hap2. Functional characterization revealed that *FtNAC2* promotes quercetin accumulation in Tartary buckwheat hairy roots and potentially serves as a multifunctional regulator influencing both drought tolerance in buckwheat and seed size in *Arabidopsis*. Transcriptome co-clustering and pull-down mass spectrometry (MS) indicated *FtNAC52* as a potential regulatory partner of *FtNAC2*. DNA affinity purification sequencing (DAP-seq) and quantitative reverse transcription PCR (qRT-PCR) analyses demonstrated that *FtNAC2* promoted quercetin biosynthesis by upregulating *FtF3'H* and *FtF3'5'H* genes. Collectively, our results elucidated how *FtNAC2* influences quercetin content variation in Tartary buckwheat, providing molecular insights into

the differential quercetin accumulation between cultivated populations.

Key words: Tartary buckwheat, quercetin, promoter variation

Introduction

Quercetin, a flavonoid involved in the phenylpropanoid pathway, is widely distributed in vegetables, fruits, cereals, and medicinal plants, serving as an essential dietary component with significant nutraceutical value (Ho et al., 2024). This bioactive compound indeed exhibits diverse pharmacological properties including antioxidant, anti-inflammatory, anti-diabetic, anti-cancer, and immunomodulatory activities, making it a potent therapeutic agent and health-promoting phytochemical (Babaei et al., 2018; Eisvand et al., 2022; Gogoi et al., 2024). While the pharmacological potential of quercetin is constrained in humans by its limited solubility and bioavailability, its metabolic effectiveness is markedly improved through natural dietary consumption (Alizadeh et al., 2023; Frenț et al., 2024). Consequently, enhancing quercetin biosynthesis in edible crops represents a viable strategy to address this pharmacological challenge (Mirsafaei et al., 2020).

In plants, quercetin plays multifaceted roles in modulating developmental processes, stress responses, and signaling pathways (Singh et al., 2021). This flavonoid functions as a potent osmoprotectant, notably mitigating mannitol-induced osmotic stress to maintain seed germination viability in Apocynum species (*A. venetum* and *A. pictum*) (Yang et al., 2021). Under environmental stresses, quercetin regulates reactive oxygen species (ROS) homeostasis and subsequently modulates phytohormone signaling, particularly auxin and abscisic acid (ABA) pathways (Peer and Murphy, 2007; Brunetti et al., 2018; Jin et al., 2025).

Quercetin biosynthesis is regulated by transcription factors (TFs). For instance, the R2R3-MYB transcription factor CitPH4 activates structural genes (*CHS*, *CHI*, and *FMO1*) to promote quercetin, pipolic acid (Pip), and N-hydroxypipecolic acid (NHP) biosynthesis in citrus (He et al., 2022; Huang et al., 2023; Lu et al., 2025). VvbZIP22 enhances quercetin accumulation in grape by directly activating the flavonol synthase gene (Liu et al., 2025). In tomato, SNAC4/9 negatively regulates quercetin levels through modulation of phenylpropanoid pathway genes (Sun et al., 2025). These transcription factors collectively determine the interspecies difference in quercetin abundance, highlighting the sophisticated mechanisms of this nutritionally important metabolite.

Buckwheat (*Fagopyrum spp.*), an ancient pseudocereal crop, has gained increasing attention due to its exceptional nutritional and medicinal value (Kreft et al., 2020). Among its two major cultivated species, Tartary buckwheat ((*F. tataricum*)) is particularly prized as a superior source of bioactive flavonoids, including quercetin and rutin, compared to common buckwheat (*F. esculentum*) (Zhu, 2016; Luthar et al., 2021; Ding et al., 2022; Zhao et al., 2023). Previous studies have revealed that Tartary buckwheat originated in the Himalayan region before undergoing two independent

domestication events that gave rise to distinct southwestern (SL) and northern (NL) landraces (Zhang et al., 2021). During range expansion, environmental heterogeneity has driven adaptive divergence between these populations. For instance, there are significant differences in precipitation and temperature between northern and southern China, resulting in higher soil salinity in northern China than in southern China (Liu and Wang, 2021). Notably, the higher soil salinity characteristic of northern regions appears to have selected for increased frequency of high-expression *FtPK* haplotypes, explaining the enhanced salt tolerance observed in northern landraces compared to their southern counterparts (He et al., 2024). This adaptive radiation has been also accompanied by genetic differentiation and concomitant metabolic reorganization of seed storage compounds (Zhao et al., 2023; He et al., 2024). While several subpopulation-specific metabolites (e.g., emodin and salicylic acid) showing differential accumulation patterns have been genetically characterized (Zhao et al., 2023), the molecular mechanisms underlying quercetin accumulation remain unexplored, representing a critical knowledge gap in understanding how genetic information shapes this nutritionally vital pathway.

Building upon previous genome-wide association study (GWAS) of quercetin content in 480 Tartary buckwheat accessions, we identified *FtNAC2* as a transcriptional activator. Haplotype analysis and luciferase reporter assays provided preliminary evidence linking promoter variations to quercetin accumulation. Functional validation through genetic transformation in Tartary buckwheat hairy roots and *A. thaliana* confirmed its regulatory role. To unravel the molecular mechanisms, we employed pull-down mass spectrometry, transcriptome co-expression analysis, and fluorescence-based screening to identify potential interactors of *FtNAC2*. Furthermore, DAP-seq coupled with qRT-PCR analysis revealed its downstream target genes. This study not only provides novel genetic insights into quercetin difference among buckwheat subspecies, but also facilitate the development of elite germplasm resources with enhanced nutritional value.

Materials and methods

Plant materials

Tissue samples were collected from two-month-old Tartary buckwheat (Fagopyrum tataricum cv. 'Pinku') plants grown in a controlled greenhouse (16-h light/8-h dark, 25°C, 60% humidity). Three biological replicates (n=3) were analyzed per treatment, following standardized protocols (Hou et al., 2021). For hairy root transformation experiments, we utilized two-week-old tissue-cultured 'Pinku' seedlings. *A. thaliana* ecotype Columbia-0 (Col-0) served as plant transformation vector.

Genome-Wide Association Analysis (GWAS)

GWAS was performed following previously described methodologies (Zhang et al., 2021). Candidate genes were identified within 100 kb flanking regions of significant loci, based on the genome-wide linkage disequilibrium (LD) decay distance. Haplotype analysis of candidate genes was conducted using Candihap software (Gao et al., 2024).

Phylogenetic tree construction

Phylogenetic analysis of NAC TFs was performed using protein sequences retrieved from UniProt. Multiple sequence alignment was conducted with Clustal W in MEGA7.0, followed by phylogenetic tree construction using the neighbor-joining method with 1000 bootstrap replicates. The resulting tree was visualized and annotated using the iTOL online platform (https://itol.embl.de/).

Subcellular localization

The *FtNAC2* gene, devoid of the stop codon, was cloned into the pCAMBIA1305 plasmid. The resulting recombinant plasmid was then transferred into *Agrobacterium tumefaciens* GV3101. Agrobacterium harboring the empty pCAMBIA1305 plasmid served as the negative control, while Agrobacterium carrying the pCAMBIA1300-mCherry-NLS (Nuclear Localization Sequence) plasmid acted as the positive marker. Subsequent experimental procedures followed the established protocols (Lai et al., 2024). Primers are shown in Table S21.

Yeast self-activation assay

Full-length and truncated sequences of *FtNAC2* (1-161aa, 1-399aa, 1-539aa) were cloned downstream of the GAL4 domain in the pGBKT7 plasmid and co-transfected into the Y2HGold strain along with an empty pGADT7 plasmid. The transformants were grown on minimal synthetic defined (SD) medium lacking leucine (L) and tryptophan (T) for 2-3 days. Positive transformants were then selected and transferred to SD/-LTHA medium for an additional 3-4 days. For further details, please consult the Yeastmaker™ Yeast Transformation System 2 User Manual by Clontech. Primers are shown in Table S21.

Quantitative real-time PCR

RNA extraction and cDNA synthesis were respectively performed using the RNA Easy Fast Plant Tissue RNA Extraction Kit (DP452, Tiangen) and the HiScript III 1st Strand cDNA Synthesis Kit (+gDNA wiper) (R323-01, Vazyme). Quantitative real-time PCR (qRT-PCR) was conducted with ChamQ Universal SYBR qPCR Master Mix (Q711-02, Vazyme) following the manufacturer's protocols. All experiments included three biological replicates, with primer sequences provided in Supplementary Table S21.

Hairy root transformation and metabolite analysis in Tartary buckwheat:

The full-length coding sequence was cloned into the pCAMBIA1307 vector and transformed into *Agrobacterium rhizogenes* strain. Hairy roots produced after transformation of *A. rhizogenes* without plasmid served as negative control A4. Hairy root induction, selection, and subculture were performed as previously described (Zhou et al., 2017; Zhang et al., 2018; Li et al., 2019). Positive transgenic lines were cultured in liquid MS medium for 15-20 days prior to flavonoid quantification using established protocols (Gao et al., 2025). For LC-MS analysis, aliquots of the same samples used for gene relative expression detection were analyzed using an Agilent G6500 series HPLC-QQQ mass spectrometer, with three biological replicates performed for each sample to ensure data reliability.

Arabidopsis transformation and seeds phenotype characterization

For overexpression lines, the full-length CDS was inserted into pCAMBIA1307 and introduced into *Agrobacterium tumefaciens* GV3101. *Arabidopsis thaliana* (Col-0) transformation was performed via the floral dip method (Clough and Bent, 1998), with positive transformants selected on 60 μg/mL hygromycin (He et al., 2024). The T-DNA insertion mutants (*anac078*, SALK_025098) was obtained from the Arashare database (https://www.arashare.cn/).

Mature dry seeds were imaged using a Zeiss stereo microscope (Carl Zeiss Microscopy GmbH), with randomly selected seeds from each line measured across three independent biological replicates at least. Seed weight was determined by weighing 100 seeds using a precision analytical balance (0.1 mg resolution). Quantitative seed phenotype analysis was performed using ImageJ software (Schneider et al., 2012).

Drought stress

For osmotic stress assays, 3-5 day-old *Arabidopsis* seedlings germinated on 1/2 MS medium were vertically transferred to fresh plates containing either control (1/2 MS) or treatment (1/2 MS + 150 mM mannitol) media. To maintain experimental consistency, all media were prepared in a single batch. Each plate contained four genotypes: one wild-type (Col-0) control and three independent overexpression lines, with three uniformly germinated seedlings per genotype. Root elongation was quantified after 7-14 days of growth. The experimental design included ≥10 replicate plates per condition, with three independent biological replicates performed.

For drought stress experiments, *Arabidopsis* seedlings were first grown on 1/2 MS medium for 10 days before being transplanted to soil and maintained under controlled environmental conditions (25°C, 16-h photoperiod, 60-80% relative humidity). Following a 2-3 week establishment period, plants were subjected to progressive drought stress by complete water withdrawal after one final thorough watering. Stress development was monitored daily through visual assessment of phenotypic markers including wilting, leaf curling, and chlorosis progression. Tissue sampling was conducted when the majority of plants exhibited pronounced wilting symptoms (typically after 10-14 days of water deprivation), with no rehydration intervention prior to collection. The experiment included photographic documentation of stress phenotypes at key developmental stages.

For hairy root culture and PEG treatment, uniform 2-cm Tartary buckwheat hairy roots were maintained in MS liquid medium with or without 20% (w/v) PEG-6000 under constant agitation (120 rpm) at 25°C. Following 20-30 days of culture, root tissues were harvested for subsequent molecular and Hydroponic Stress Treatment

For hydroponic stress treatment, seven-day-old hydroponically-grown buckwheat seedlings were subjected to osmotic stress by treatment with 20% PEG-6000 under controlled growth conditions (25°C, 16-h photoperiod). Tissue samples were collected at specified time intervals (0, 1, 3, and 6 h post-treatment), immediately frozen in liquid N_2, and stored at -80°C until processing. Three

independent biological replicates were included for each time point.

Physiological measurements

Fresh tissue samples (0.1 g) were snap-frozen in liquid nitrogen and homogenized to a fine powder in 2 mL microcentrifuge tubes. Subsequently, malondialdehyde (MDA; Solarbio, BC0025), catalase (CAT; Solarbio, BC0205), and superoxide dismutase (SOD; Solarbio, BC0175) contents were quantified using commercially available assay kits according to the manufacturer's specifications. The experiment included three independent biological replicates.

Fluorescence signal assay

The target promoter sequence and TFs respectively were cloned into the pGreen II 0800-LUC and pGreen II 62-sk reporter vector for dual-luciferase reporter gene assay, and the fluorescence complementation experiments were performed using pCAMBIA1300-cLuc and pCAMBIA1300-nLuc vectors. The primer sequences were provided in table S21. Recombinant vectors were transformed into *A. tumefaciens* strain GV3101 and cultured at 28°C. For transient expression assays, Agrobacterium cultures were infiltrated into leaves of 4-week-old *Nicotiana benthamiana* plants. Infiltrated plants were first incubated in darkness for 24 h, followed by 48 h under long-day conditions (16-h light/8-h dark photoperiod at 23°C/22°C day/night temperature). Luminescence detection was performed by applying 3 mg/ml D-luciferin potassium salt substrate evenly to the infiltrated leaf areas under dim light. After 5 min of dark adaptation, luminescent signals were captured using a charge-coupled device (CCD) imaging system (Plant In Vivo Imaging System).

Protein-protein interaction (PPI) prediction and 3D structure visualization

Protein-protein interaction predictions were generated using AlphaFold Server (https://alphafoldserver.com/welcome), followed by structural visualization and analysis with PyMOL Molecular Graphics System (v2.5.0).

Potential interacting proteins identified by pull-down MS were analyzed using the STRING database (https://stringdb.org/cgi/input?sessionId=bSiH2mgRfaXL&input_page_show_search=on) to construct a PPI network with *A. thaliana* as the reference organism. The resulting network was visualized and further analyzed using software Cytoscape 3.9.1.

Prokaryotic expression and GST pull-down assays:

The coding sequence corresponding to the conserved domain (amino acids 1-182) of *FtNAC2* was cloned into the pGEX-4T-1 expression vector. The recombinant plasmid was transformed into *Escherichia coli* Transetta (DE3) competent cells (CD801-02, TransGen Biotech) for protein expression. The GST-tagged fusion protein (GST-FtNAC21-182) was purified using glutathione sepharose affinity chromatography. Total protein extracts from Tartary buckwheat were prepared using a Plant Protein Extraction Kit (BC3720, Solarbio). For pull-down assays, the plant protein extracts were incubated with purified GST-FtNAC2$^{1-182}$ fusion protein, with GST protein alone serving as a negative control. The protein mixtures were then applied to glutathione sepharose

columns for affinity purification. After extensive washing to remove nonspecifically bound proteins, the GST-tagged protein complexes were eluted. The eluted samples were separated by SDS-PAGE and visualized by coomassie brilliant blue staining. Differential protein bands were excised for subsequent mass spectrometry analysis, which was performed according to the methodology previously at the ZHONG DA Platform Center of Crop Science Research Institute, Chinese Academy of Agricultural Sciences (He et al., 2023). The relevant primers were shown in table S21.

Transcriptome co-expression cluster analysis

Gene expression patterns for 20% PEG-6000 transcriptome of Tartary buckwheat were analyzed using co-clustering approaches implemented in the R package TCseq (Li et al., 2018; Lai et al., 2024). Heat map drawing was completed using TBtools software (Chen et al., 2020).

DAP-seq assay

The full-length coding sequence of *FtNAC2* was cloned into the pUC57-HALO vector to generate an N-terminal HALO-tagged fusion protein. HALO-FtNAC2 protein was synthesized *in vitro* using 500 ng of pUC57-HALO-FtNAC2 plasmid and the TNT SP6 Coupled Reticulocyte Lysate System (Promega), following the manufacturer's protocol. The expressed protein was immediately incubated with 10 μL Magne-HALO Tag beads (Promega) in 1× phosphate-buffered saline (PBS) containing 0.005% (v/v) Nonidet P-40 and 0.1% (v/v) Tween-20 at 25°C for 1 h. After five washes with PBS containing 0.1% Tween-20 (PBST), bead-bound proteins were treated with DNase I to remove contaminating DNA. For DNA-binding assays, the DNA-free HALO-FtNAC2 protein was incubated with 500 μg of sonicated genomic DNA (300-500 bp fragments) from Tartary buckwheat cultivar 'Pinku' at 25°C for 1 h. Following eight stringent washes with PBST, bound DNA was eluted using elution buffer at 98°C for 10 min. Sequencing libraries were prepared from the eluted DNA using the TruePrep DNA Library Prep Kit V2 for Illumina (Vazyme), with paired-end sequencing performed by Annoroad Gene Technology (Beijing). Data analysis was conducted as previously described (Li et al., 2024).

KEGG enrichment analysis

Gene ontology and pathway enrichment analyses were conducted through the OmicShare online platform (v8.3) with KEGG pathway database (Release 106.0). The analysis employed Fisher's exact test with genome-wide annotation as reference background, followed by multiple testing correction using the Benjamini-Hochberg procedure. Statistically significant pathways were identified at a false discovery rate (FDR) threshold of 5% (q-value < 0.05).

Statistical analysis

Statistical analyses were performed using GraphPad Prism 10.1.2, including Pearson correlation ($P < 0.05$), Student's t-tests, and one-way ANOVA ($P < 0.05$). Data are presented as mean ± standard deviation (SD) from three independent biological replicates ($n = 3$), and significance levels denoted as $^{*}P < 0.05$, $^{**}P < 0.01$, and $^{***}P < 0.001$. Data visualization was generated using the same software – Graphpad Prism 10.1.2, with detailed statistical results provided in Supplementary Table.

Omics data

The metabolome and transcriptome (accession number: PRJCA003569) of Tartary buckwheat were obtained from previous studies (Huang et al., 2021; Zhao et al., 2022).

Results

Identification of *FtNAC2* based on the GWAS of quercetin content

The previous genome-wide resequencing and population structure analysis of *F. tataricum* accessions identified two distinct landraces, SL (Southwestern landraces) and NL (Northern landraces), derived from wild progenitor HW (Himalayan wild accessions) through independent domestication events (Zhang et al., 2021). Here, we now report significant metabolic divergence between these two landraces subspecies. Comparative profiling revealed markedly higher quercetin accumulation in NL landraces compared to SL (Figure 1a) (Zhang et al., 2021), suggesting that the domestication signatures are associated with quercetin divergence and potentially led to subspecies differentiation in quercetin content.

Genome-wide association analysis of quercetin content across 480 Tartary buckwheat accessions identified two significant loci on chromosomes 1 and 3, containing 18 and 12 putative genes respectively (Figure 1b, S1, Table S1) (Zhang et al., 2021). Building upon the observed divergence in drought tolerance indices (membership function value analysis, MVDF) between SL and NL populations (Figure 1c, Table S2), we conducted a comprehensive transcriptomic analysis of GWAS-identified candidate genes under PEG-induced osmotic stress to explore their potential roles in drought adaptation. Transcriptomic analysis under 20% PEG-6000-induced drought stress identified four rapidly responsive genes (*FtPinG0303189600*; *FtPinG0303190200*; *FtPinG0100938900* and *FtPinG0303190600*), among which the NAC domain-containing protein (FtPinG0303190600) showed the most significant induction (especially at 1 h post-treatment; Figure 1d-e, Table S1) (Huang et al., 2021). The remaining two early-response genes, encoding uncharacterized proteins with no known functional domains (Table S1), were excluded from further investigation due to their undefined biological relevance. Phylogenetic analysis classified this transcription factor within the NAC2 subfamily, showing closest homology to *Arabidopsis ANAC053* (locus name: *At3g10500*, 36.9% identity/51.5% similarity) and *ANAC078* (locus name: *At5g04410*, 37.5% identity/51.3% similarity) (Figures 1f-g, S2), leading to its designation as *FtNAC2*. As *ANAC078* is implicated in regulating flavonoid pathway gene expression in response to light stress in *Arabidopsis* (Morishita et al., 2009), we proposed that *FtNAC2* likely functions as a regulatory component in quercetin biosynthesis in Tartary buckwheat.

Promoter variation modulates *FtNAC2* expression

Genomic sequence analysis of *FtNAC2* across diverse accessions revealed multiple SNP variations distributed as follows: upstream (11 SNPs), intergenic regions (10 SNPs), introns (6 SNPs), exonic regions (2 SNPs) and downstream (2 SNPs) (Table S3). Notably, two polymorphic sites in the

promoter region segregated 453 accessions into three predominant haplotypes (Hap1, Hap2, and Hap3; Figure 2a, Table S3). Comparative analysis revealed significantly lower quercetin content in Hap1 compared to Hap2, while neither haplotype differing significantly from Hap3 (Figure 2b, Table S3). Haplotype distribution revealed striking population-specific patterns: Hap1 predominated in southern cultivated (SL) accessions (72.4% frequency) (Figure 2c), whereas Hap2 was prevalent in northern (NL) populations (61.95%) (Figure 2d). These findings suggest that the observed differential accumulation of quercetin between SL and NL populations (Figure 1a) may be associated with promoter polymorphisms in *FtNAC2*, potentially contributing to the ecotype-specific flavonoid biosynthesis regulation.

To better understand the role of the promoter in quercetin accumulation, we examined the promoter activity of the two haplotypes. Cloning of the 2-kb promoter regions (ATG upstream) from both haplotypes into the 0800-LUC reporter system showed higher fluorescence signal for the Hap.2 (Figure 2e-f, Table S4). Further analysis of expression profiling of *FtNAC2* across diverse accessions further revealed significantly higher transcript abundance in Hap2 carriers compared to Hap1 (Figure 2g, Table S5), suggesting that promoter polymorphisms between these haplotypes differentially regulate *FtNAC2* expression levels. These findings collectively suggest that haplotype-specific promoter activity variations modulate *FtNAC2* expression levels, and that *FtNAC2* functions as a potential positive regulator of quercetin biosynthesis in Tartary buckwheat.

In addition, bioinformatic analysis using PlantPAN 4.0 predicted that promoter SNPs may disrupt transcription factor (TF) binding motifs, with SNP^{-980} located within putative binding sites for NAC, C3H, ERF, and Dof families, while SNP^{-505} potentially affects bZIP, Trihelix, and LBD TF binding (Figure 2a, Table S6). Notably, SNP^{-980} contained the highest number of predicted NAC family binding sequences (n=24) (Table S6), prompting focused investigation of NAC-mediated regulatory networks in subsequent analyses.

Characterisation and expression analysis of *FtNAC2*

Subcellular localization assays in tobacco (*Nicotiana benthamiana*) revealed that *FtNAC2* predominantly localizes to the nucleus, with minor cytoplasmic distribution (Figure 3a), consistent with its predicted function as a transcription factor. Protein domain analysis confirmed the presence of a conserved ~150-amino acid NAC domain at the N-terminus (characteristic of the NAC TF family) and variable transcriptional activation domain in protein interactions and DNA binding (Figure S2; Puranik et al., 2012). Yeast transactivation assays demonstrated that while various truncated constructs grew normally under double-dropout conditions, only yeast expressing full-length and 1-539aa survived on quadruple-dropout medium (Figure 3b-c). Notably, deletion of the C-terminal region (amino acids 399-621) completely abolished transcriptional activation capacity (Figure 3b-c), providing direct evidence that *FtNAC2* functions as a transcriptional activator and that its transactivation domain resides in the C-terminus.

The difference in gene expression levels in various tissues and treatments reflects its specialized functional roles (Li et al., 2018; Liu et al., 2019). Quantitative analysis revealed highest *FtNAC2* transcript abundance in roots, followed by flowers and seeds, with lower expression in stems and leaves (Figure 3d, Table S7). Treatment of Tartary buckwheat seedlings with 20% PEG-6000 elicited a pronounced stress response, characterized by significant upregulation of *FtNAC2* transcript levels at 3 h post-treatment (Figure 3e, Table S7). Although the magnitude of induction differed from observations in the PEG transcriptome data, *FtNAC2* was consistently induced under osmotic stress and exhibited a sustained expression pattern, suggesting its potential functional role in drought adaptation mechanisms. Furthermore, analysis of MVDF and quercetin content datasets revealed a positive correlation (Figure 3f, Table S2) (He et al., 2024), combined with the contribution of quercetin antioxidant capacity to environmental stress tolerance (Brunetti et al., 2018), which supports a potential linkage between quercetin abundance and drought adaptation.

FtNAC2 overexpression promoted quercetin accumulation and enhanced drought tolerance in Tartary buckwheat hairy roots

To investigate the role of *FtNAC2* in quercetin biosynthesis, we established transgenic hairy roots of Tartary buckwheat. Metabolite profiling of positive transgenic lines (OE lines) (Figure S3a, Table S8) demonstrated that *FtNAC2* overexpression significantly enhanced both total flavonoid content (Figure 4a, Table S8) and increased quercetin accumulation (Figure 4b, Table S9), which is consistent with our previous haplotype analysis (Figure 2b, 2g). Comprehensive metabolic analysis revealed coordinated changes across the phenylpropanoid pathway, as some downstream flavonoids (catechin, epicatechin, and proanthocyanidins) showed moderate increases, while observing significant reductions in several precursor (L-phenylalanine and naringenin) and flavonoid glycosides (kaempferol-3-glucoside and cyanidin-3-glucoside; Figure 4b, Table S9). These findings established *FtNAC2* as a key regulator that not only promoted quercetin biosynthesis but may also interfered with the synthesis of other substances in the phenylpropanoid pathway.

Given the significant induction of *FtNAC2* by 20% PEG-6000, we assessed its functional role under osmotic stress. While no phenotypic differences were observed between control A4 (*A. rhizogenes* 4) and OE lines under normal MS medium conditions (Figure 4c-d, Table S10), PEG-6000 treatment revealed that OE lines accumulated significantly higher biomass than controls (Figure 4c, e, Table S10). This enhanced stress tolerance was associated with increased activities of key antioxidant enzymes (Catalase, CAT and Superoxide dismutase, SOD) (Figure 4f-g, Table S10) and reduced malondialdehyde (MDA) (Figure 4h, Table S10) levels in OE lines, indicating improved cellular protection against oxidative damage. Building on the well-documented antioxidant properties of quercetin and its established role in abiotic stress responses (Singh et al., 2021), we propose that *FtNAC2* enhances plant stress tolerance through a dual mechanism: (1) upregulation of quercetin biosynthesis and (2) modulation of peroxidase activity to improve reactive oxygen species (ROS)

scavenging capacity.

Regulatory network mediated by *FtNAC2*

Transcription factors frequently form protein complexes to execute their biological functions, making protein-protein interaction (PPI) network analysis crucial for understanding complex regulatory processes. To identify potential FtNAC2 interacting proteins, we performed *in vitro* pull-down assays using GST-FtNAC2 as bait with GST alone serving as negative control, followed by mass spectrometry analysis that identified 588 candidate interacting proteins (Table S11). Following FPKM-based filtering of master proteins identified by mass spectrometry, we retained 546 highly expressed candidates for STRING database analysis. The resulting PPI network revealed specific interactions between FtNAC2 and only two NAC family members in Tartary buckwheat: *FtPinG0303261500* (named FtNAC52) and *FtPinG0809107800* (named FtNAC8) (Figure 5a, Table S12). Co-expression analysis demonstrated that *FtNAC52* clustered with *FtNAC2* in 20% PEG-6000 transcriptome (Figure5b, Table S13), while AlphaFold Server predictions identified extensive hydrogen bonding between these two proteins, suggesting strong molecular interactions (Figure 5c). This was further confirmed by fluorescence complementation experiments and Tartary buckwheat hairy root overexpression (Figure 5d-f, Table S14), indicating that *FtNAC52* is an interacting factor of *FtNAC2* and that their interaction leads to upregulated expression of *FtNAC2*.

We previously noted that SNP^{-980} variation potentially leads to mutations in NAC family binding elements (Figure 5g, Table S4). Thus, we employed AlphaFold modeling to predict the interaction between FtNAC52 protein and the binding sequence at the *FtNAC2* promoter SNP^{-980} site. The simulation results showed that there were multiple hydrogen bonding forces between the FtNAC52 protein and the putative binding sequence, indicating potential interaction between them (Figure 5h, Table S4). Next, we tested the ability of FtNAC52 to activate the two promoters. Dual-luciferase assays further demonstrated significantly stronger activation of the $Hap2^{pro}$ variant by FtNAC52 compared to $Hap1^{pro}$ (Figure 5i-j, Table S15), supporting the existence of a dual interaction mechanism, in which FtNAC52 protein can not only interact with the FtNAC2, but also regulate the expression of *FtNAC2* through promoter binding. The mutation of the NAC binding element caused by the variation of promoter SNPs potentially affects the regulatory effect of FtNAC52 on the *FtNAC2* promoter, ultimately showing differences in gene expression and quercetin content between populations.

Identification of *FtNAC2* binding targets by DAP-seq

Transcription factors exert their regulatory functions primarily through binding to promoter regions of downstream target genes, with their genomic binding profiles reflecting biological activities. Our DNA affinity purification sequencing (DAP-seq) analysis identified 33,398 putative *FtNAC2* binding peaks ($p<0.01$) distributed across the Tartary buckwheat genome (Figure S4), with 17.57% located within 2 kb upstream of transcription start sites (TSS), 3.25% in exonic regions, and 68.45% in intergenic regions (Figure 6a, Table S16). Motif analysis revealed significant enrichment of the

mitochondrial dysfunction motif (MDM) "TTNNNNNNCAA/CG" (E-value = 1×10^{-495}), along with several NAC recognition sequence (NACRS)-like motifs including "CTCACGCAAT" (E-value = 1×10^{-68}), "GTGCACGATTCT" (E-value = 1×10^{-52}), and "CGTC/GAT/CGC" (E-value = 1×10^{-25}) (Figure 6b).

KEGG enrichment analysis of promoter-bound targets showed predominant association with metabolic pathways, particularly secondary metabolite biosynthesis, but also with MAPK cascades, plant hormone signaling, plant-pathogen interaction, and with the metabolic processes of carbon metabolism, sugar and amino acid (Figure 6c, Table S17). These findings position *FtNAC2* as a key regulator of flavonoid biosynthesis through targeted promoter binding. Notably, genes associated with the quercetin biosynthetic pathway were significantly enriched in the phenylpropanoid metabolism, including key enzymes such as 4-coumarate-CoA ligase (4CL), cinnamate 4-hydroxylase (C4H), phenylalanine ammonia-lyase (PAL), cytochrome P450s (CYP450s), glycosyltransferases (GTs), and methyltransferase (MTs) (Table S17). Quercetin biosynthesis involves multiple CYP450 oxygenases: flavonol synthase (FLS) mediates dihydroquercetin reduction, flavonoid 3'-hydroxylase (F3'H) catalyzes kaempferol hydroxylation, and flavonoid 3',5'-hydroxylase (F3'5'H) converts quercetin to myricetin. Additionally, UDP-glycosyltransferase (UFGT) converts quercetin to its glycosylated form, isoquercetin (Figure 6d). Through systematic analysis of DAP-seq binding peaks in promoter regions, we identified three key flavonoid biosynthesis-related genes as potential targets of *FtNAC2*: Two cytochrome P450 genes - *FtPinG0302524300* (*FtF3'H*) and *FtPinG0707657000* (*FtF3'5'H*), One glycosyltransferase gene - *FtPinG0707621700* (*FtUFGT*). Gene expression analysis in *FtNAC2* transgenic hairy roots showed significant upregulation of *FtF3'H* and *FtF3'5'H* alongside downregulation of *FtUFGT* (Figures 6e-g, Table S8). Promoter activity assays further verified that *FtNAC2* activates *CYP450* genes while repressing glycosyltransferase expression (Figure 6h-j, Table S18), revealing its dual regulatory function in enhancing quercetin biosynthesis while restricting its glycosylation. These findings suggest that *FtNAC2* regulates gene expression by targeting the promoters of enzyme genes in the metabolite synthesis pathway, thereby regulating quercetin accumulation.

FtNAC2 is a multifunctional gene with the potential to regulate the balance between yield and quality of Tartary buckwheat

We also simultaneously overexpressed *FtNAC2* in *Arabidopsis* when we explored the function. Overexpression of *FtNAC2* in transgenic *Arabidopsis* led to the coordinated upregulation of core phenylpropanoid biosynthetic genes, including phenylalanine ammonia-lyase (*AtPAL*), chalcone synthase (*AtCHS*), flavonol synthase (*AtFLS*), and flavanone 3-hydroxylase (*AtF3H*), thus consistently demonstrating the role of this gene in phenylpropanoid metabolism (Figure S5, Table S19). When 3-day-old seedlings were transferred to 150 mM mannitol plates to induce osmotic stress, *FtNAC2*-overexpressing (OE) lines exhibited significantly longer roots than wild-type (WT) controls (Figure 7a-d, Table S19). Under natural drought conditions, OE lines maintained greener

stems and higher survival rates compared to WT plants showing typical stress symptoms (e.g., wilting, leaf yellowing; Figure 7e-f, Table S19). Consistent with the enhanced stress tolerance observed in Tartary buckwheat, OE lines showed nearly 2-fold higher catalase (CAT) and superoxide dismutase (SOD) activities, along with about 15-20% reduced malondialdehyde (MDA) content relative to WT under drought stress (Figure 7g-I, Table S19), further confirming the role of *FtNAC2* in alleviating drought stress.

Unexpectedly, OE lines produced significantly smaller seeds than Col-0, with reductions in length (nearly 11%), width (approximately 15%), and hundred-seed weight (about 15%) (Figure 7j-m, S6, Table S17). Conversely, *ANAC078* knockout (KO) lines - the *Arabidopsis* homologs exhibiting highest sequence identity to *FtNAC2* - displayed increased seed dimensions (nearly 8% length and 9% width) though hundred-seed weight remained unchanged (Figure 7j-m, S7, Table S20). This inverse phenotypic relationship between OE and KO lines suggests *FtNAC2* may coordinate trade-offs between stress adaptation and reproductive allocation in plants.

Discussion

Buckwheat is believed to have originated in the Tibetan Plateau or mountainous regions near Yunnan in southwestern China (Ohnishi, 1998; Tsuji and Ohnishi, 2001; Ohnishi and Konishi, 2021; Fan et al., 2020). Previous studies have demonstrated distinct geographic distribution patterns between the SL and NL populations, with non-overlapping domestication processes indicating these genetically and geographically differentiated subspecies underwent independent domestication events (Zhang et al., 2021). Subsequent research revealed extensive metabolic divergence between domesticated SL and NL subspecies, suggesting these subspecies-specific metabolites may reflect underlying genetic differentiation (Zhao et al., 2023). Recent genomic evidence indicates that cultivated buckwheat diverged from the HW group approximately 2,028-5,814 years ago, followed by the subsequent differentiation of SL and NL groups between 1,450-4,411 years before present (He et al., 2024). Our findings extend this understanding by identifying significant variation in quercetin content between SL and NL populations (Figure 1a), with GWAS analysis linking this metabolic variation to the *FtNAC2* locus (Figures 1b-c, S1, Table S1). Haplotype analysis showed predominant Hap2 haplotype in NL populations versus Hap1 dominance in SL (Figure 2c-d, Table S2), a genetic divergence potentially associated with geographic adaptation and human dietary preferences (Song and Cho, 2017; Song et al., 2022; Wang et al., 2023; Jiao et al., 2023).

In fact, The distinct climatic patterns between northern and southern China, shaped by latitude, topography, and monsoon influences, have led to marked differences in both environmental conditions and dietary habits (He, 2022). Climatic patterns in northern China are characterized by concentrated summer precipitation events of shorter duration compared to southern regions, with significantly lower annual rainfall totals and heightened vulnerability to spring drought conditions. In contrast, southern China experiences prolonged rainy seasons accompanied by the distinctive

mei-yu front phenomenon, resulting in substantially greater annual precipitation (Zhan et al., 2021; Li et al., 2023) (https://data.cma.cn/). These environmental contrasts are reflected in regional cuisines: northern diets emphasize robust flavors with higher oil and salt content, serving dual purposes of meeting elevated caloric demands and addressing seasonal food scarcity, particularly during winter months, whereas southern culinary traditions favor lighter, sweeter profiles adapted to the humid subtropical climate (Zhang and Ma, 2020). Given quercetin's dual roles in environmental stress tolerance and bitter taste perception (Lu et al., 2025), its differential accumulation likely influences both local adaptation and culinary characteristics, leading to distinct genetic preservation under natural and artificial selection (Singh et al., 2021; Kreft et al., 2022; Zhao et al., 2024; Zhao et al., 2025).

Protein-protein interactions critically regulate cellular functions (Ding et al., 2014; Hasan et al., 2023). Our PPI analysis and pull-down-MS identified FtNAC52 as potential *FtNAC2* interactor (Figure 5a-d, Table S11-13), and further prediction of binding sequence of *FtNAC2* promoter variant site revealed that *FtNAC52* potential serves dual regulatory roles - both as an interacting partner of FtNAC2 and as a transcriptional activator of its promoter (Figure 5e-j, Table S14-15). While the precise molecular mechanisms underlying FtNAC52-FtNAC2 regulation extend beyond the scope of this study, their coordinated influence on population-specific gene expression patterns suggests potential contributions to Tartary buckwheat subspecies differentiation that warrant further investigation. In addition, our transcriptome co-cluster analysis revealed two ubiquitin ligase among *FtNAC2* potential targets (Figure 5b, Table S13, S22), consistent with reported functions of its *Arabidopsis* ortholog *ANAC78*. In *Arabidopsis*, NAC78 forms homo- or heterodimers with NAC53 to regulate proteotoxic stress responses as a key component of the proteasome stress regulon (PSR) through 26S proteasome involvement (Gladman et al., 2016). Similarly, rice OsNAC78 interacts with OsNACIP6 to activate *OsGSTU37* expression, thereby enhancing drought tolerance through ROS scavenging (Yu et al., 2024). These parallel findings across diverse species suggest evolutionary conservation of functional mechanisms among NAC78 orthologs, including *FtNAC2* in Tartary buckwheat.

Transcriptional regulation primarily occurs through cis-element binding (Ma et al., 2024). Our DAP-seq analysis revealed strong MDM motif enrichment (Figure 6b), consistent with NAC53/NAC78 studies (Lee et al., 2012; De Clercq et al., 2013; Gladman et al., 2016). Previous studies have identified the PRCE element (consensus core: TGGGC) as the preferential binding site for NAC78 (Yabuta et al., 2010; Nguyen et al., 2013). However, our motif enrichment analysis of *FtNAC2* binding peaks did not significantly enrich this sequence, suggesting potential functional divergence in DNA recognition among NAC family members. Moreover, our analysis identified multiple NAC recognition sequence (NACRS) core motifs (Figure 6b), indicating that *FtNAC2* likely regulates an extensive network of downstream target genes involved in diverse biological pathways beyond secondary metabolite biosynthesis.

In functional genetic studies, *Arabidopsis* serves as a commonly utilized model system for heterologous gene expression (Yaschenko et al., 2025). Our results demonstrate that *FtNAC2* overexpression enhances drought tolerance in both Tartary buckwheat (Figure 4c-e, Table S10) and *Arabidopsis* (Figure 7a-f, Table S19). However, we unexpectedly observed significantly reduced seed size in transgenic *Arabidopsis* lines (Figure 7j-m, S6, Table S20), suggesting FtNAC2 may function as a multifunctional regulator. In addition, we observed that the T-DNA insertion lines exhibited modest increases in seed size without corresponding changes in seed weight, suggesting species-specific functional diversification of this NAC regulator. Notably, this uncoupling of size-weight relationships contrasts with canonical seed development patterns where testa and endosperm growth are tightly coordinated, as demonstrated in *Arabidopsis arf2* mutants where increased testa cell numbers elevate both size and mass (Okushima et al., 2005; Hughes et al., 2008; Orozco-Arroyo et al., 2015). The observed phenotypic dissociation may reflect differential regulation of size-determining pathways (e.g., IKU, ubiquitin-proteasome, G-protein, MAPK signaling, and phytohormonal networks) versus storage product biosynthesis (starch/protein/lipid metabolism and transport) (Li and Li, 2015; Li and Li, 2016; Ren et al., 2019; Ren et al., 2023). While most studies report coupled size-weight changes, our findings highlight an exceptional case meriting further investigation.

While the current limitations in buckwheat stable genetic transformation efficiency restricted our seed phenotype analysis to *Arabidopsis*, we observed that Hap2 accessions with higher quercetin content exhibited significantly lower thousand-seed weight (TSW) compared to Hap1 in Tartary buckwheat (Figure S8, Table S3), consistent with the *Arabidopsis* transgenic phenotype showing reduced seed dimensions in *FtNAC2*-overexpressing lines (Figure 7a-m, Table S20). Therefore, we speculated that *FtNAC2* may play an important role in the balance between yield and quality of Tartary buckwheat. While the robust antioxidant capacity of quercetin has been well-documented in plant stress responses, this metabolic adaptation simultaneously imposes constraints on reproductive fitness (Fini et al., 2012; Singh et al., 2021). Under natural selection pressures, plants employ sophisticated regulatory mechanisms to optimize the allocation of finite metabolic resources between growth and stress response pathways (Ali and Baloch, 2020; Wang et al., 2020), exemplified by OsNAC120 balancing GA-mediated growth and ABA-induced drought tolerance in rice (Xie et al., 2024), and CaNAC2c physically interacting with CaHSP70 and CaNAC029 in a context-specific manner to coordinate fruit development with stress responses in pepper (Cai et al., 2021). Such physiological trade-offs represent evolutionary adaptations to maximize fitness in challenging environments. We propose a model wherein *FtNAC2* fine-tunes resource allocation as an adaptive strategy, preferentially enhancing stress responses at the potential cost of reproductive growth (Figure 8), though the precise molecular mechanisms underlying this potential growth-defense trade-off require further elucidation.

Collectively, while *FtNAC2* shares sequence similarity and conserved domains with *Arabidopsis*

ANAC078 and *ANAC053*, we identified significant divergence in its C-terminal regions (Figure S2), suggesting that group-specific motifs within the transcription regulatory regions (TRRs) may confer functional specialization in biological processes (Jensen et al., 2010; Puranik et al., 2012; Xiong et al., 2025). This specialization pattern potentially mirrors the functional diversification observed among NAC homologs in other species: *OsNAC78*-mediated drought tolerance in rice (Yu et al., 2024), *ZmNAC7*-regulated iron homeostasis in maize (Yan et al., 2023), and *ANAC07*8-dependent flavonoid induction under high-light stress in *Arabidopsis* (Morishita et al., 2009). Herein, we provides the first mechanistic evidence that *FtNAC2* promoter polymorphisms drive quercetin accumulation divergence between Tartary buckwheat subspecies (SL vs. NL), potential linking genetic variation to adaptive traits including drought tolerance, yield potential, and flavor profiles. These findings establish a new paradigm for NAC-mediated metabolic adaptation in non-model crops. Discovery of an distinct regulatory module through the identification of *FtNAC52* as a novel *FtNAC2* interactor, which orchestrates flavonoid biosynthesis independently of known *Arabidopsis* (*ANAC078*) or rice (*OsNAC78*) pathways. The haplotype-discriminative markers (Hap1/Hap2; Figure 2) enable precision engineering of stress-resilient, nutritionally enhanced buckwheat cultivars.

Author contributions

M.Z., M.-L.F., G.P., and K.Z. conceived and designed the study. J.W., W.L., D.F., Y.S., and H.L. performed the experiments and conducted data analysis. J.W., W.L.and Y.H. wrote the original manuscript draft. M.-L.F., G.P., M.Q., M.G., K.Z., and M.Z. critically reviewed and revised the manuscript. All authors read and approved the final version of the manuscript for publication.

Acknowledgments

This work was supported by the National Key Research and Development Program of China (Grant No. 2023YFD1200701) and the National High-level University Graduate Scholarship Program of the China Scholarship Council (Award No. 202303250057).

Conflict of interest statement

The authors declare no competing interests.

Data availability statement

The metabolome and transcriptome (accession number: PRJCA003569) of Tartary buckwheat were retrieved from the publications (Huang et al., 2021; Zhao et al., 2022). The DAP-seq data from this work were submitted to the China National Center for Bioinformation (CNCB) Genome Sequence Archive and are publicly accessible under the accession code PRJCA046210.

Supporting information

All supporting data are included in the manuscript and its supplementary materials.

Figure S1 Genome-wide association study (GWAS) of quercetin content in Tartary buckwheat.

Figure S2 Multiple sequence alignment of NAC transcription factors.

Figure S3 Transcript abundance of *FtNAC2* in Tartary buckwheat hairy root overexpression lines.

Figure S4 Distribution of *FtNAC2* binding peaks across the whole buckwheat genome using DAP-seq. Ft1-8 represent the eight chromosomes of buckwheat. NAC-DAP narrowPeak indicates the distribution of binding gaps compared to the control, and pinku.gff indicates the gene density at each chromosome position.

Figure S5 Relative expression analysis of gene in transgenic *Arabidopsis* lines.

Figure S6 Seed morphology analysis of *Arabidopsis thaliana*.

Figure S7 Gel electrophoresis images of PCR genotyping of Arabidopsis thaliana ANAC078 T-DNA inserted lines.

Figure S8 Comparison of 1000-grain weight of Tartary buckwheat between Hap1 and Hap2.

Table S1 Intervals of Quercetin content GWAS for 480 Tartary buckwheat on Chr3.

Table S2 Quercetin content (QC, mg/g) and MFVD of 240 Tartary buckwheat.

Table S3 Quercetin content and 1000-grain-weight of three Haplotype in Tartary buckwheat.

Table S4 LUC/REN of Hap1 and Hap2 promoter by dual fluorescence signal detection.

Table S5 Relative expression of *FtNAC2* in germplasms with different haplotypes.

Table S6 The prediction results of CREs of *FtNAC2* promoter.

Table S7 Relative expression of *FtNAC2* in Tartary buckwheat.

Table S8 Gene relative expression in *FtNAC2*-OE lines in hairy root.

Table S9 Flavonoids content (mg/g) of hairy root.

Table S10 Fresh weight and physiological indicators under 20% PEG treatment of hairy root.

Table S11 Potential target proteins identified by pull-down.

Table S12 Gene ID of PPI network.

Table S13 Co-cluster analysis of 20% PEG-6000 transcriptome.

Table S14 Gene relative expression in *FtNAC52*-OE lines in Tartary buckwheat hairy root.

Table S15 LUC/REN values of *FtNAC52* binding to different haplotype promoters of *FtNAC2*.

Table S16 DAP-seq binding site information of *FtNAC2*.

Table S17 KEGG enrichment analysis of promoter binding peak of *FtNAC2*.

Table S18 LUC/REN of *FtNAC2* binding to *FtF3'5'H*, *FtF3'H* and *FtUFGT* promoter.

Table S19 Relative expression, survival rate and root length under 150 mM mannitol treatment of *Arabidopsis*.

Table S20 Transgenic *Arabidopsis* phenotype.

Table S21 Primer list.

Table S22 Gene information co-clustered with *FtNAC2* in the PEG transcriptome and identified by pull-down-MS.

References

Ali, S., Baloch, A.M. (2020) Overview of sustainable plant growth and differentiation and the role of hormones in controlling growth and development of plants under various stresses. Recent Pat. Food Nutr. Agric. 11, 105–114. https://doi.org/10.2174/2212798410666190619104712

Alizadeh, S.R., Savadkouhi, N., Ebrahimzadeh, M.A. (2023) Drug design strategies that aim to improve the low solubility and poor bioavailability conundrum in quercetin derivatives. Expert Opin. Drug Discov. 18, 1117–1132. https://doi.org/10.1080/17460441.2023.2241366

Babaei, F., Mirzababaei, M., Nassiri-Asl, M. (2018) Quercetin in food: possible mechanisms of its effect on memory. J. Food Sci. 83, 2280–2287. https://doi.org/10.1111/1750-3841.14317

Bian, H., Song, P., Gao, Y., Deng, Z., Huang, C., Yu, L., Wang, H., Ye, B., Cai, Z., Pan, Y., Wang, F., Liu, J., Gao, X., Chen, K., Jia, G., Klee, H.J., Zhang, B. (2024) The m6A reader SlYTH2 negatively regulates tomato fruit aroma by impeding the translation process. Proc. Natl. Acad. Sci. 121, e2405100121. https://doi.org/10.1073/pnas.2405100121

Brunetti, C., Fini, A., Sebastiani, F., Gori, A., Tattini, M. (2018) Modulation of phytohormone signaling: a primary function of flavonoids in plant–environment interactions. Front. Plant Sci. 9. https://doi.org/10.3389/fpls.2018.01042

Cai, J., Panda, S., Kazachkova, Y., Amzallag, E., Li, Z., Meir, S., Rogachev, I., Aharoni, A. (2024) A NAC triad modulates plant immunity by negatively regulating N-hydroxy pipecolic acid biosynthesis. Nat. Commun. 15, 7212. https://doi.org/10.1038/s41467-024-51515-2

Cai, W., Yang, S., Wu, R., Cao, J., Shen, L., Guan, D., Shuilin, H. (2021) Pepper NAC-type transcription factor NAC2c balances the trade-off between growth and defense responses. Plant Physiol. 186, 2169–2189. https://doi.org/10.1093/plphys/kiab190

Chen, C., Chen, H., Zhang, Y., Thomas, H.R., Frank, M.H., He, Y., Xia, R. (2020) TBtools: an integrative toolkit developed for interactive analyses of big biological data. Mol. Plant 13, 1194–1202. https://doi.org/10.1016/j.molp.2020.06.009

Chen, Y., Xia, P. (2025) NAC transcription factors as biological macromolecules responded to abiotic stress: a comprehensive review. Int. J. Biol. Macromol. 308, 142400. https://doi.org/10.1016/j.ijbiomac.2025.142400

Clough, S.J., Bent, A.F. (1998) Floral dip: a simplified method for -mediated transformation of. Plant J. 16, 735–743.

https://doi.org/10.1046/j.1365-313x.1998.00343.x

De Clercq, I., Vermeirssen, V., Van Aken, O., Vandepoele, K., Murcha, M.W., Law, S.R., Inzé, A., Ng, S., Ivanova, A., Rombaut, D., van de Cotte, B., Jaspers, P., Van de Peer, Y., Kangasjärvi, J., Whelan, J., Van Breusegem, F. (2013) The membrane-bound NAC transcription factor ANAC013 functions in mitochondrial retrograde regulation of the oxidative stress response in *Arabidopsis*. Plant Cell 25, 3472–3490. https://doi.org/10.1105/tpc.113.117168

Diao, P., Chen ,Chong, Zhang ,Yuzhen, Meng ,Qingwei, Lv ,Wei, and Ma, N. (2020) The role of NAC transcription factor in plant cold response. Plant Signal. Behav. 15, 1785668. https://doi.org/10.1080/15592324.2020.1785668

Ding, M., He, Y., Zhang, K., Li, J., Shi, Y., Zhao, M., Meng, Y., Georgiev, M.I., Zhou, M. (2022) JA-induced *FtBPM3* accumulation promotes FtERF-EAR3 degradation and rutin biosynthesis in Tartary buckwheat. Plant J. 111, 323–334. https://doi.org/10.1111/tpj.15800

Ding, Y.-D., Chang, J.-W., Guo, J., Chen, D., Li, S., Xu, Q., Deng, X.-X., Cheng, Y.-J., Chen, L.-L. (2014) Prediction and functional analysis of the sweet orange protein-protein interaction network. BMC Plant Biol. 14, 213. https://doi.org/10.1186/s12870-014-0213-7

Duval, M., Hsieh, T.-F., Kim, S.Y., Thomas, T.L. (2002) Molecular characterization of *AtNAM*: a member of the *Arabidopsis* NAC domain superfamily. Plant Mol. Biol. 50, 237–248. https://doi.org/10.1023/A:1016028530943

Eisvand, F., Tajbakhsh, A., Seidel, V., Zirak, M.R., Tabeshpour, J., Shakeri, A. (2022) Quercetin and its role in modulating endoplasmic reticulum stress: A review. Phytother. Res. 36, 73–84. https://doi.org/10.1002/ptr.7283

Fan, Y., Ding, M., Zhang, K., Tang, Y., Fang, W., Yang, K., Zhang, Z., Cheng, J., Zhou, M. (2020) Overview and utilization of wild germplasm resources of the genus *Fagopyrum Mill.* In Chinese. J Plant Genet Resour. 21, 1395–406.

Fini, A., Guidi, L., Ferrini, F., Brunetti, C., Di Ferdinando, M., Biricolti, S., Pollastri, S., Calamai, L., Tattini, M. (2012) Drought stress has contrasting effects on antioxidant enzymes activity and phenylpropanoid biosynthesis in Fraxinus ornus leaves: an excess light stress affair? J. Plant Physiol. 169, 929–939. https://doi.org/10.1016/j.jplph.2012.02.014

Frenț, O.-D., Stefan, L., Morgovan, C.M., Duteanu, N., Dejeu, I.L., Marian, E., Vicaș, L., Manole, F. (2024) A systematic review: quercetin-secondary metabolite of the flavonol class, with multiple health benefits and low bioavailability. Int. J. Mol. Sci. 25, 12091. https://doi.org/10.3390/ijms252212091

Fuertes-Aguilar, J., Matilla, A.J. (2024) Transcriptional control of seed life: new insights into the role of the NAC family. Int. J. Mol. Sci. 25, 5369. https://doi.org/10.3390/ijms25105369

Gao, Y., Shi, Y., Jahan, T., Huda, Md.N., Hao, L., He, Y., Quinet, M., Chen, H., Zhang, K., Zhou, M. (2025) Buckwheat UDP-glycosyltransferase *FtUGT71K6* and *FtUGT71K7* tandem repeats contribute to drought tolerance by regulating epicatechin synthesis. Plant Cell Environ. n/a. https://doi.org/10.1111/pce.15412

Gladman, N.P., Marshall, R.S., Lee, K.-H., Vierstra, R.D. (2016) The proteasome stress regulon is controlled by a pair of NAC

transcription factors in *Arabidopsis*. Plant Cell 28, 1279–1296. https://doi.org/10.1105/tpc.15.01022

Gogoi, D., Chattopadhyay, P., Dolui, S.K., Khan, M.R., Mukherjee, A.K. (2024) Studies on *in vivo* antithrombotic activity of quercetin, a natural flavonoid isolated from a traditional medicinal plant, African eggplant (*Solanum indicum*). J. Ethnopharmacol. 335, 118686. https://doi.org/10.1016/j.jep.2024.118686

Hasan, M., Kumar, N., Majeed, A., Ahmad, A., Mukhtar, S. (2023) Protein–protein interaction network analysis using networkX, in: Mukhtar, S. (Ed.), Protein-Protein Interactions: Methods and Protocols. Springer US, New York, NY, pp. 457–467. https://doi.org/10.1007/978-1-0716-3327-4_35

He, J., Xu, Y., Huang, D., Fu, J., Liu, Z., Wang, L., Zhang, Y., Xu, R., Li, L., Deng, X., Xu, Q. (2022) TRIPTYCHON-LIKE regulates aspects of both fruit flavor and color in citrus. J. Exp. Bot. 73, 3610–3624. https://doi.org/10.1093/jxb/erac069

He, J., Hao, Y., He, Y., Li, W., Shi, Y., Khurshid, M., Lai, D., Ma, C., Wang, X., Li, J., Cheng, J., Fernie, A.R., Ruan, J., Zhang, K., Zhou, M. (2024) Genome-wide associated study identifies *FtPMEI13* gene conferring drought resistance in Tartary buckwheat. Plant J. 120, 2398–2419. https://doi.org/10.1111/tpj.17119

He, X. (2022) Northern and southern China: regional differences in rural areas. eBook ISBN 9781003182757. https://doi.org/10.4324/9781003182757

He, Y., Zhang, K., Li, S., Lu, X., Zhao, H., Guan, C., Huang, X., Shi, Y., Kang, Z., Fan, Y., Li, W., Chen, C., Li, G., Long, O., Chen, Y., Hu, M., Cheng, J., Xu, B., Chapman, M.A., Georgiev, M.I., Fernie, A.R., Zhou, M. (2023) Multiomics analysis reveals the molecular mechanisms underlying virulence in Rhizoctonia and jasmonic acid-mediated resistance in Tartary buckwheat (*Fagopyrum tataricum*). Plant Cell 35, 2773–2798. https://doi.org/10.1093/plcell/koad118

He, Y., Zhang, K., Shi, Y., Lin, H., Huang, X., Lu, X., Wang, Z., Li, W., Feng, X., Shi, T., Chen, Q., Wang, J., Tang, Y., Chapman, M.A., Germ, M., Luthar, Z., Kreft, I., Janovská, D., Meglič, V., Woo, S.-H., Quinet, M., Fernie, A.R., Liu, X., Zhou, M. (2024) Genomic insight into the origin, domestication, dispersal, diversification and human selection of Tartary buckwheat. Genome Biol. 25, 61. https://doi.org/10.1186/s13059-024-03203-z

Ho, W.-Y., Shen, Z., Chen, Y., Chen, T.-H., Lu, X., Fu, Y.-S. (2024) Therapeutic implications of quercetin and its derived-products in COVID-19 protection and prophylactic. Heliyon 10. https://doi.org/10.1016/j.heliyon.2024.e30080

Hou, S., Du, W., Hao, Y., Han, Y., Li, H., Liu, L., Zhang, K., Zhou, M., Sun, Z. (2021) Elucidation of the regulatory network of flavonoid biosynthesis by profiling the metabolome and transcriptome in Tartary buckwheat. J. Agric. Food Chem. 69, 7218–7229. https://doi.org/10.1021/acs.jafc.1c00190

Huang, J., Chen, Qijiao, Rong, Y., Tang, B., Zhu, L., Ren, R., Shi, T., Chen, Qingfu. (2021) Transcriptome analysis revealed gene regulatory network involved in PEG-induced drought stress in Tartary buckwheat (*Fagopyrum tararicum*). PeerJ 9, e11136. https://doi.org/10.7717/peerj.11136

Huang, Y., He, J., Xu, Y., Zheng, W., Wang, S., Chen, P., Zeng, B., Yang, S., Jiang, X., Liu, Zishuang, Wang, L., Wang, X., Liu, S., Lu, Z., Liu, Ziang, Yu, H., Yue, J., Gao, J., Zhou, X., Long, C., Zeng, X., Guo, Y.-J., Zhang, W.-F., Xie, Z., Li, C., Ma, Z., Jiao, W., Zhang, F., Larkin, R.M., Krueger, R.R., Smith, M.W., Ming, R., Deng, X., Xu, Q. (2023) Pangenome analysis provides insight into the evolution of the orange subfamily and a key gene for citric acid accumulation in citrus fruits. Nat. Genet. 55, 1964–1975. https://doi.org/10.1038/s41588-023-01516-6Hughes, R., Spielman, M., Schruff, M.C., Larson, T.R., Graham, I.A., Scott, R.J., 2008. Yield assessment of integument-led seed growth following targeted repair of auxin response factor 2. Plant Biotechnol. J. 6, 758–769. https://doi.org/10.1111/j.1467-7652.2008.00359.x

Jensen, M.K., Kjaersgaard, T., Nielsen, M.M., Galberg, P., Petersen, K., O'Shea, C., Skriver, K. (2010) The Arabidopsis thaliana NAC transcription factor family: structure–function relationships and determinants of ANAC019 stress signalling. Biochem. J. 426, 183–196. https://doi.org/10.1042/BJ20091234

Jiao, Y., Jiang, H., Li, W., Wang, L., Wang, S., Jia, X., Wang, Z., Wang, H., Zhang, B., Ding, G. (2023) Analysis of differentiated regional dietary patterns of adults aged 18-64 years in 15 provinces (autonomous regions, municipalities) in 2018. Wei Sheng Yan Jiu 52, 11–19. https://doi.org/10.19813/j.cnki.weishengyanjiu.2023.01.003

Jin, Y., Yan, H., Zhu, X., Yang, Y., Jia, J., Sun, M., Najeeb, A., Luo, J., Wang, X., He, M., Xu, B., Li, X., Luo, Z., Mao, C., Huang, D., Nie, G., Feng, G., Xie, Z., Zhang, X., Luo, L., Huang, L. (2025) Single-cell transcriptomes reveal spatiotemporal heat stress response in pearl millet leaves. New Phytol. 247, 637–650. https://doi.org/10.1111/nph.70232

Ko, J.-H., Yang, S.H., Park, A.H., Lerouxel, O., Han, K.-H. (2007) ANAC012, a member of the plant-specific NAC transcription factor family, negatively regulates xylary fiber development in *Arabidopsis thaliana*. Plant J. 50, 1035–1048. https://doi.org/10.1111/j.1365-313X.2007.03109.x

Kreft, I., Zhou, M., Golob, A., Germ, M., Likar, M., Dziedzic, K., Luthar, Z. (2020) Breeding buckwheat for nutritional quality. Breed. Sci. 70, 67–73. https://doi.org/10.1270/jsbbs.19016

Kreft, I., Vollmannová, A., Lidiková, J., Musilová, J., Germ, M., Golob, A., Vombergar, B., Kocjan Ačko, D., Luthar, Z. (2022) Molecular shield for protection of buckwheat plants from UV-B radiation. Mol. Basel Switz. 27, 5577. https://doi.org/10.3390/molecules27175577

Lai, D., Zhang, K., He, Y., Fan, Y., Li, W., Shi, Y., Gao, Y., Huang, X., He, J., Zhao, H., Lu, X., Xiao, Y., Cheng, J., Ruan, J., Georgiev, M.I., Fernie, A.R., Zhou, M. (2024) Multi-omics identification of a key glycosyl hydrolase gene *FtGH1* involved in rutin hydrolysis in Tartary buckwheat (*Fagopyrum tataricum*). Plant Biotechnol. J. 22, 1206–1223. https://doi.org/10.1111/pbi.14259

Lee, S., Seo, P.J., Lee, H.-J., Park, C.-M. (2012) A NAC transcription factor NTL4 promotes reactive oxygen species production during drought-induced leaf senescence in *Arabidopsis*. Plant J. 70, 831–844. https://doi.org/10.1111/j.1365-313X.2012.04932.x

Li, D., Yang, J., Pak, S., Zeng, M., Sun, J., Yu, S., He, Y., Li, C. (2022) *PuC3H35* confers drought tolerance by enhancing lignin and

proanthocyanidin biosynthesis in the roots of *Populus ussuriensis*. New Phytol. 233, 390–408. https://doi.org/10.1111/nph.17799

Li, H., Lv, Q., Ma, C., Qu, J., Cai, F., Deng, J., Huang, J., Ran, P., Shi, T., Chen, Q. (2019) Metabolite profiling and transcriptome analyses provide insights into the flavonoid biosynthesis in the developing seed of Tartary buckwheat (*Fagopyrum tataricum*). J. Agric. Food Chem. 67, 11262–11276. https://doi.org/10.1021/acs.jafc.9b03135

Li, J., Zhang, K., Meng, Y., Li, Q., Ding, M., Zhou, M. (2019) *FtMYB16* interacts with Ftimportin-α1 to regulate rutin biosynthesis in Tartary buckwheat. Plant Biotechnol. J. 17, 1479–1481. https://doi.org/10.1111/pbi.13121

Li, M., Liu, J., Zhou, Y., Zhou, S., Zhang, S., Tong, H., Zhao, A. (2020) Transcriptome and metabolome profiling unveiled mechanisms of tea (*Camellia sinensis*) quality improvement by moderate drought on pre-harvest shoots. Phytochemistry 180, 112515. https://doi.org/10.1016/j.phytochem.2020.112515

Li, M., Ma, Z., Zheng, T., Sun, W., Zhang, Y., Jin, W., Zhan, J., Cai, Y., Tang, Y., Wu, Q., Tang, Z., Bu, T., Li, C., Chen, H. (2018) Insights into the correlation between physiological changes in and seed development of Tartary buckwheat (*Fagopyrum tataricum Gaertn.*). BMC Genomics. 19, 648. https://doi.org/10.1186/s12864-018-5036-8.

Li, M., Wang, G., Zong, S., Chai, X. (2023) Copula-based assessment and regionalization of drought risk in China. Int. J. Environ. Res. Public. Health 20, 4074. https://doi.org/10.3390/ijerph20054074

Li, N., Li, Y. (2015) Maternal control of seed size in plants. J. Exp. Bot. 66, 1087–1097. https://doi.org/10.1093/jxb/eru549

Li, N., Li, Y., 2016. Signaling pathways of seed size control in plants. Curr. Opin. Plant Biol., SI: 33: Cell signalling and gene regulation 2016 33, 23–32. https://doi.org/10.1016/j.pbi.2016.05.008Li, X., Li, J., Wei, S., Gao, Y., Pei, H., Geng, R., Lu, Z., Wang, P., Zhou, W. (2024) Maize GOLDEN2-LIKE proteins enhance drought tolerance in rice by promoting stomatal closure. Plant Physiol. 194, 774–786. https://doi.org/10.1093/plphys/kiad561

Liu, M., Sun, W., Ma, Z., Zheng, T., Huang, L., Wu, Q., Zhao, G., Tang, Z., Bu, T., Li, C., Chen, H. (2019) Genome-wide investigation of the AP2/ERF gene family in Tartary buckwheat (*Fagopyum tataricum*). BMC Plant Biol. 19, 84. https://doi.org/10.1186/s12870-019-1681-6

Liu L, Wang B. (2021) Protection of halophytes and their uses for cultivation of saline-alkali soil in China. Biology (Basel). 10:353–5. https://doi.org/10.3390/biology10050353Liu, G., Zhang, Z., Tian, Y., Yang, J., Xu, X., Liu, X. (2025) *VvbZIP22* regulates quercetin synthesis to enhances cold resistance in grape. Plant Sci. 350, 112293. https://doi.org/10.1016/j.plantsci.2024.112293

Lu, L., Fang, J., Xia, N., Zhang, J., Diao, Z., Wang, X., Liu, Y., Tang, D., Li, S. (2025) Phosphorylation of the transcription factor OsNAC29 by OsMAPK3 activates diterpenoid genes to promote rice immunity. Plant Cell 37, koae320. https://doi.org/10.1093/plcell/koae320

Luthar, Z., Zhou, M., Golob, A., Germ, M. (2021) Breeding buckwheat for increased levels and improved quality of protein. Plants 10, 14. https://doi.org/10.3390/plants10010014

Ma, Z., Hu, L., Jiang, W. (2024) Understanding AP2/ERF transcription factor responses and tolerance to various abiotic stresses in plants: a comprehensive review. Int. J. Mol. Sci. 25, 893. https://doi.org/10.3390/ijms25020893

Mirsafaei, L., Reiner, Ž., Shafabakhsh, R., Asemi, Z. (2020) Molecular and biological functions of quercetin as a natural solution for cardiovascular disease prevention and treatment. Plant Foods Hum. Nutr. Dordr. Neth. 75, 307–315. https://doi.org/10.1007/s11130-020-00832-0

Morishita, T., Kojima, Y., Maruta, T., Nishizawa-Yokoi, A., Yabuta, Y., Shigeoka, S. (2009) *Arabidopsis* NAC transcription factor, ANAC078, regulates flavonoid biosynthesis under high-light. Plant Cell Physiol. 50, 2210–2222. https://doi.org/10.1093/pcp/pcp159

Nguyen, H.M., Schippers, J.H.M., Gõni-Ramos, O., Christoph, M.P., Dortay, H., van der Hoorn, R.A.L., Mueller-Roeber, B. (2013) An upstream regulator of the 26S proteasome modulates organ size in rabidopsis thaliana. Plant J. 74, 25–36. https://doi.org/10.1111/tpj.12097

Nuruzzaman, M., Sharoni, A.M., Kikuchi, S. (2013) Roles of NAC transcription factors in the regulation of biotic and abiotic stress responses in plants. Front. Microbiol. 4. https://doi.org/10.3389/fmicb.2013.00248

Ohnishi, O. (1998) Search for the wild ancestor of buckwheat III. The wild ancestor of cultivated common buckwheat, and of Tatary buckwheat. Econ Bot. 52, 123–33.

Ohnishi, O., Konishi, T. (2001) Cultivated and wild buckwheat species in eastern Tibet. 18, 3–8.

Okushima, Y., Mitina, I., Quach, H.L., Theologis, A. (2005) AUXIN RESPONSE FACTOR 2 (ARF2): a pleiotropic developmental regulator. Plant J 43:29–46. doi:10.1111/j.1365-313X.2005.02426.x

Orozco-Arroyo, G., Paolo, D., Ezquer, I., Colombo, L. (2015) Networks controlling seed size in Arabidopsis. Plant Reprod. 28, 17–32. https://doi.org/10.1007/s00497-015-0255-5

Peer, W.A., Murphy, A.S. (2007) Flavonoids and auxin transport: modulators or regulators? Trends Plant Sci. 12, 556–563. https://doi.org/10.1016/j.tplants.2007.10.003

Puranik, S., Sahu, P.P., Srivastava, P.S., Prasad, M. (2012) NAC proteins: regulation and role in stress tolerance. Trends Plant Sci. 17, 369–381. https://doi.org/10.1016/j.tplants.2012.02.004

Raza, A., Charagh, S., Zahid, Z., Mubarik, M.S., Javed, R., Siddiqui, M.H., Hasanuzzaman, M. (2021) Jasmonic acid: a key frontier in conferring abiotic stress tolerance in plants. Plant Cell Rep. 40, 1513–1541. https://doi.org/10.1007/s00299-020-02614-z

Ren, D., Ding, C., Qian, Q. (2023) Molecular bases of rice grain size and quality for optimized productivity. Sci. Bull. 68, 314–350. https://doi.org/10.1016/j.scib.2023.01.026

Ren, D., Wang, X., Yang, M., Yang, L., He, G., Deng, X.W. (2019) A new regulator of seed size control in Arabidopsis identified by a genome-wide association study. New Phytol. 222, 895–906. https://doi.org/10.1111/nph.15642Schneider, C.A., Rasband, W.S., Eliceiri, K.W. (2012) NIH image to imageJ: 25 years of image analysis. Nat. Methods 9, 671–675. https://doi.org/10.1038/nmeth.2089

Selth, L.A., Dogra, S.C., Rasheed, M.S., Healy, H., Randles, J.W., Rezaian, M.A. (2005) A NAC domain protein interacts with tomato leaf curl virus replication accessory protein and enhances viral replication. Plant Cell 17, 311–325. https://doi.org/10.1105/tpc.104.027235

Shang, Y., Ma, Y., Zhou, Y., Zhang, H., Duan, L., Chen, H., Zeng, J., Zhou, Q., Wang, S., Gu, W., Liu, M., Ren, J., Gu, X., Zhang, S., Wang, Y., Yasukawa, K., Bouwmeester, H.J., Qi, X., Zhang, Z., Lucas, W.J., Huang, S. (2014) Biosynthesis, regulation, and domestication of bitterness in cucumber. Science 346, 1084–1088. https://doi.org/10.1126/science.1259215

Singh, P., Arif, Y., Bajguz, A., Hayat, S. (2021) The role of quercetin in plants. Plant Physiol. Biochem. PPB 166, 10–19. https://doi.org/10.1016/j.plaphy.2021.05.023

Song, F., Cho, M.S. (2017) Geography of food consumption patterns between south and north China. Foods 6, 34. https://doi.org/10.3390/foods6050034

Song, Y., Feng, J., Liu, D., Long, C. (2022) Different phenylalanine pathway responses to cold stress based on metabolomics and transcriptomics in Tartary buckwheat landraces. J. Agric. Food Chem. 70, 687–698. https://doi.org/10.1021/acs.jafc.1c06915

Souer, E., van Houwelingen, A., Kloos, D., Mol, J., Koes, R. (1996) *The no apical meristem* gene of petunia ss required for pattern formation in embryos and flowers and is expressed at meristem and primordia boundaries. Cell. 85, 159–170. https://doi.org/10.1016/S0092-8674(00)81093-4

Sun, Y., Huang, Z., Zhao, X., Qiao, L., Xue, Z., Gao, R., Peng, B., Wu, C., Kou, X. (2025) Combined analysis of transcriptomics and metabolomics showed that SNAC4 and SNAC9 are negative regulators of the resistance to *Botrytis cinerea* in tomato. Plant Physiol. Biochem. 219, 109447. https://doi.org/10.1016/j.plaphy.2024.109447

Tsuji, K., Ohnishi, O. (2001) Phylogenetic relationships among wild and cultivated Tartary buckwheat (*Fagopyrum tataricum Gaert.*) populations revealed by AFLP analyses. Genes Genet. Syst. 76, 47–52. https://doi.org/10.1266/ggs.76.47

Wang, C., Sheng, Q., Zhao, R., Zhu, Z. (2023) Differences in the suitable distribution area between northern and southern China landscape plants. Plants 12, 2710. https://doi.org/10.3390/plants12142710

Wang, Q., Yu, F., Xie, Q. (2020) Balancing growth and adaptation to stress: crosstalk between brassinosteroid and abscisic acid signaling. Plant Cell Environ. 43, 2325–2335. https://doi.org/10.1111/pce.13846

Xie, Z., Jin, L., Sun, Y., Zhan, C., Tang, S., Qin, T., Liu, N., Huang, J. (2024) *OsNAC120* balances plant growth and drought tolerance by integrating GA and ABA signaling in rice. Plant Commun. 5, 100782. https://doi.org/10.1016/j.xplc.2023.100782

Xiong, H., He, H., Chang, Y., Miao, B., Liu, Z., Wang, Q., Dong, F., Xiong, L. (2025) Multiple roles of NAC transcription factors in plant development and stress responses. J. Integr. Plant Biol. 67, 510–538. https://doi.org/10.1111/jipb.13854

Xu, B., Ohtani, M., Yamaguchi, M., Toyooka, K., Wakazaki, M., Sato, M., Kubo, M., Nakano, Y., Sano, R., Hiwatashi, Y., Murata, T., Kurata, T., Yoneda, A., Kato, K., Hasebe, M., Demura, T. (2014) Contribution of NAC transcription factors to plant *Adaptation* to

817 Land. Science 343, 1505–1508. https://doi.org/10.1126/science.1248417

818 Yabuta, Y., Morishita ,Teruyuki, Kojima ,Yusuke, Maruta ,Takanori, Nishizawa-Yokoi ,Ayako, and Shigeoka, S. (2010) Identification of
819 recognition sequence of ANAC078 protein by the cyclic amplification and selection of targets technique. Plant Signal. Behav. 5, 695–
820 697. https://doi.org/10.4161/psb.5.6.11577

821 Yan, P., Du, Q., Chen, H., Guo, Z., Wang, Z., Tang, J., Li, W.-X. (2023) Biofortification of iron content by regulating a NAC transcription
822 factor in maize. Science 382, 1159–1165. https://doi.org/10.1126/science.adf3256

823 Yang, J., Zhang, L., Jiang, L., Zhan, Y.G., Fan, G.Z. (2021) Quercetin alleviates seed germination and growth inhibition in *Apocynum*
824 *venetum* and *Apocynum pictum* under mannitol-induced osmotic stress. Plant Physiol. Biochem. PPB 159, 268–276.
825 https://doi.org/10.1016/j.plaphy.2020.12.025

826 Yaschenko, A.E., Alonso, J.M., Stepanova, A.N. (2025) *Arabidopsis* as a model for translational research. Plant Cell 37, koae065.
827 https://doi.org/10.1093/plcell/koae065

828 Yu, X., Xie, Y., Wang, L., Li, L., Jiang, S., Zhu, Y., Xie, Hongguang, Cui, L., Wei, Y., Xiao, Y., Cai, Q., Zheng, Y., Chen, L., Xie, Huaan,
829 Zhang, J. (2024) Transcription factor NAC78 cooperates with NAC78 interacting protein 6 to confer drought tolerance in rice. Plant
830 Physiol. 196, 1642–1658. https://doi.org/10.1093/plphys/kiae395

831 Zhan, Y., Ju, X., Fan, S., Zhou, Z., Tang, G., Ren, G. (2021) An analysis of minute summer precipitation in China during 1965—2019.
832 Acta Meteorologica Sinica, 79(4): 598-611.

833 Zhang, J., Lyu, H., Chen, J., Cao, X., Du, R., Ma, L., Wang, N., Zhu, Z., Rao, J., Wang, J., Zhong, K., Lyu, Y., Wang, Y., Lin, T., Zhou,
834 Yao, Zhou, Yongfeng, Zhu, G., Fei, Z., Klee, H., Huang, S. (2024) Releasing a sugar brake generates sweeter tomato without yield
835 penalty. Nature 635, 647–656. https://doi.org/10.1038/s41586-024-08186-2

836 Zhang, K., Logacheva, M.D., Meng, Y., Hu, J., Wan, D., Li, L., Janovská, D., Wang, Z., Georgiev, M.I., Yu, Z., Yang, F., Yan, M., Zhou,
837 M. (2018) Jasmonate-responsive MYB factors spatially repress rutin biosynthesis in *Fagopyrum tataricum*. J. Exp. Bot. 69, 1955–
838 1966. https://doi.org/10.1093/jxb/ery032

839 Zhang, K., He, M., Fan, Y., Zhao, H., Gao, B., Yang, K., Li, F., Tang, Y., Gao, Q., Lin, T., Quinet, M., Janovská, D., Meglič, V.,
840 Kwiatkowski, J., Romanova, O., Chrungoo, N., Suzuki, T., Luthar, Z., Germ, M., Woo, S.-H., Georgiev, M.I., Zhou, M. (2021)
841 Resequencing of global Tartary buckwheat accessions reveals multiple domestication events and key loci associated with agronomic
842 traits. Genome Biol. 22, 1–17. https://doi.org/10.1186/s13059-020-02217-7

843 Zhang, N., Ma, G. (2020) Nutritional characteristics and health effects of regional cuisines in China. J. Ethn. Foods 7, 1–10.
844 https://doi.org/10.1186/s42779-020-0045-z

845 Zhao, H., He, Y., Zhang, K., Li, S., Chen, Y., He, M., He, F., Gao, B., Yang, D., Fan, Y., Zhu, X., Yan, M., Giglioli-Guivarc'h, N., Hano,
846 C., Fernie, A.R., Georgiev, M.I., Janovská, D., Meglič, V., Zhou, M. (2023) Rewiring of the seed metabolome during Tartary

847 buckwheat domestication. Plant Biotechnol. J. 21, 150–164. https://doi.org/10.1111/pbi.13932

848 Zhao, H., Wang, L., Jia, Y., Zhao, J., Li, C., Chen, H., Wu, H., Wu, Q. (2024) Accumulation of the bitter substance quercetin mediated by

849 the overexpression of a novel seed-specific gene *FtRDE2* in Tartary buckwheat. Plant Physiol. Biochem. PPB 207, 108402.

850 https://doi.org/10.1016/j.plaphy.2024.108402

851 Zhao, J., Wu, H., Wang, Lijiao, Yin, Z., Sun, Y., Wang, Lei, Li, C., Zhao, H., Wu, Q. (2025) The seed-specific rutin-degrading enzyme

852 FtBGLU29 is a key factor promoting the accumulation of the bitter compound quercetin in Tartary buckwheat. J. Agric. Food Chem.

853 73, 5328–5340. https://doi.org/10.1021/acs.jafc.4c10858

854 Zhou, M., Sun, Z., Ding, M., Logacheva, M.D., Kreft, I., Wang, D., Yan, M., Shao, J., Tang, Y., Wu, Y., Zhu, X. (2017) FtSAD2 and

855 FtJAZ1 regulate activity of the FtMYB11 transcription repressor of the phenylpropanoid pathway in *Fagopyrum tataricum*. New

856 Phytol. 216, 814–828. https://doi.org/10.1111/nph.14692

857 Zhu, F. (2016) Chemical composition and health effects of Tartary buckwheat. Food Chem. 203, 231–245.

858 https://doi.org/10.1016/j.foodchem.2016.02.050

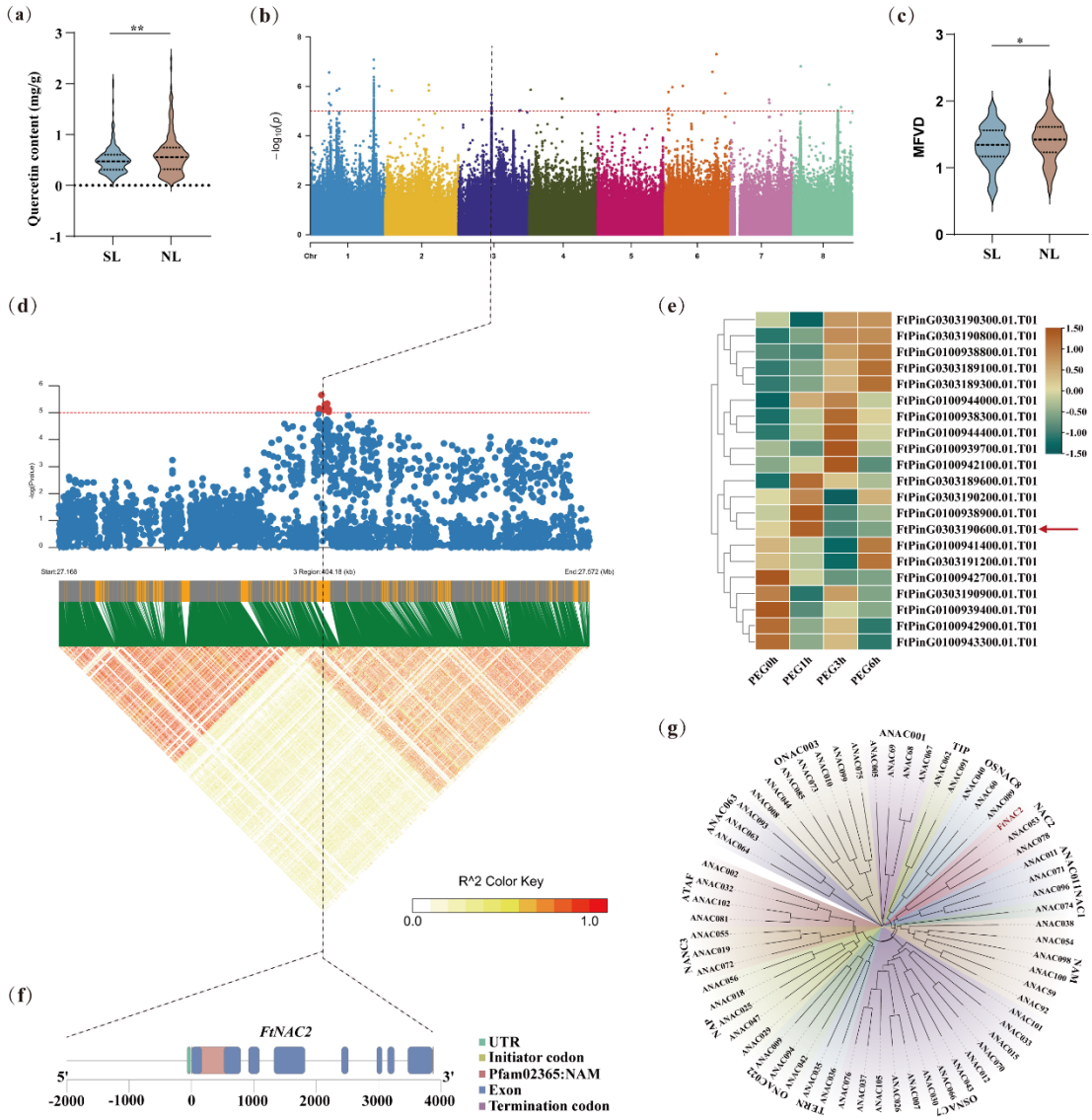

Figure 1 Identification of *FtNAC2* in Tartary buckwheat.

(a) Quercetin content among SL (Southwestern landraces) and NL (Northern landraces) groups. (b) Manhattan plot of Genome-wide association analysis (GWAS) for quercetin content of 2018zhaotong. The dashed horizontal line indicates the genome-wide significance threshold ($-\log_{10}P = 5$). (c) drought tolerance indices (membership function value analysis, MVDF) among SL and NL groups. (d) Regional manhattan map of GWAS for quercetin content. The 0.1 Mb genomic regions on either side of the most significant SNP. The lead SNP is shown in red. (e) The heatmap displays expression patterns of GWAS interval genes under osmotic stress (20% PEG-6000), which data from Huang et al., 2021. The color gradient represents relative expression levels, with warm colors indicating upregulation and cool colors indicating downregulation compared to untreated controls (0 h). (f) Gene structure information of *FtNAC2*. (g) Phylogenetic tree of FtNAC2 in Tartary buckwheat and NAC TFs in *Arabidopsis*. Data are presented as mean ± standard deviation (SD) and significance levels denoted as *P < 0.05, **P < 0.01.

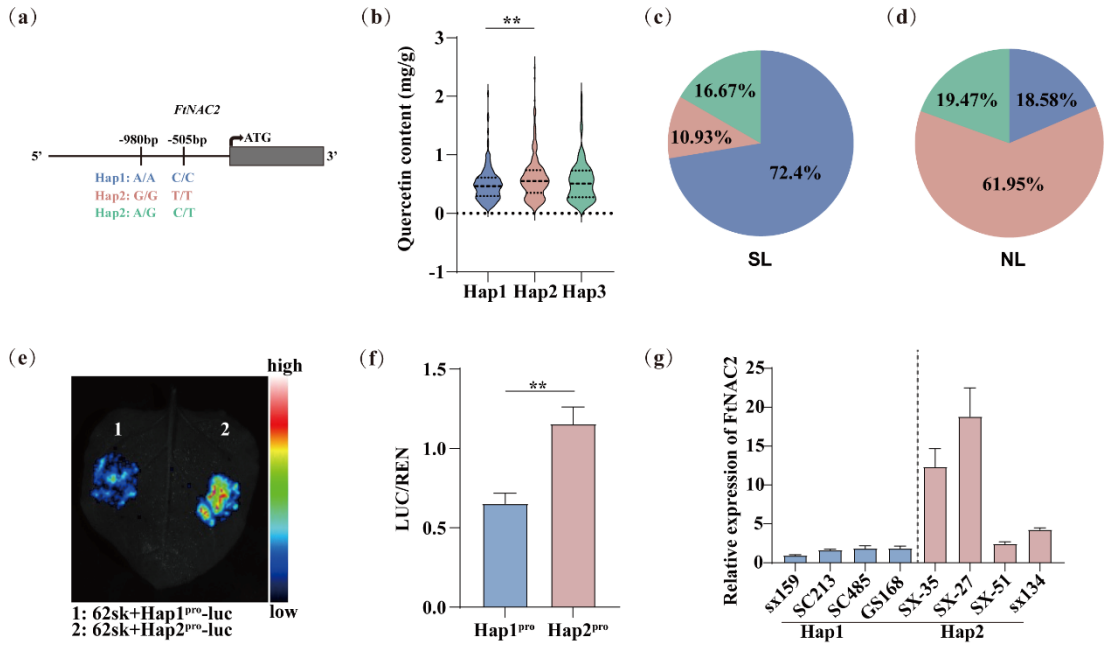

Figure 2 Haplotype differences resulting from promoter variation.

(a) Schematic representation of haplotype-defining SNPs in the *FtNAC2* promoter region. (b) Comparative analysis of quercetin content among the three major haplotypes (Hap1, Hap2, and Hap3). The proportion of the three major haplotypes in SL (c) and NL (d) populations. The haplotype distribution is color-coded as follows: Hap1 (blue), Hap2 (pink), and Hap3 (green), with each color representing a distinct haplotype group in the analyzed population. (e) Promoter fluorescence signals and (f) LUC/REN ratio of Hap1 and Hap2 variants using the 0800-LUC system. (g) Relative expression levels of *FtNAC2* in Hap1 and Hap2 accessions. Data are presented as mean ± standard deviation (SD) and significance levels denoted as **P < 0.01.

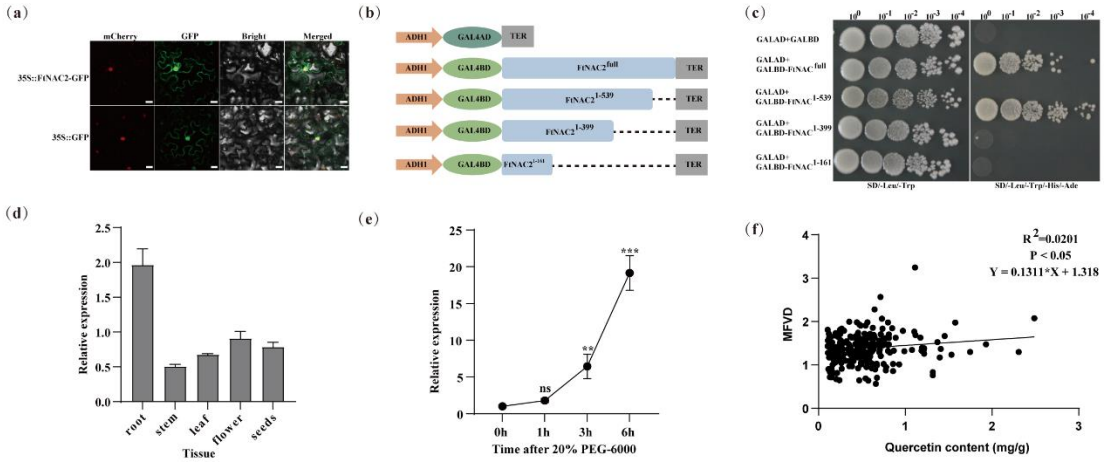

Figure 3 Functional characterization of *FtNAC2* in Tartary buckwheat.

(a) Subcellular localization of FtNAC2-GFP (green) co-expressed with the nuclear marker NLS-mCherry (red) in *N. benthamiana*. White scale bar = 20 μm. (b) Domain architecture of FtNAC2 truncation constructs. The conserved N-terminal NAC domain (amino acids 1-150) and variable C-terminal region are indicated. Dotted lines mark the deleted segments used for functional analysis. (c) Transcriptional activation assay in yeast. Protein domain annotations are indicated as follows: "full" denotes the complete amino acid sequence, while

numerical ranges (e.g., "1-539") specify the positions of inserted functional segments, with all subsequent constructs following this consistent numbering convention. (d) Tissue-specific expression profile of *FtNAC2* in Tartary buckwheat. (e) Relative expression of *FtNAC2* in Tartray buckwheat under 20% PEG-6000. Transcript levels were normalized to the reference gene *FtH3*. Data represent mean ± SD (n = 3 biological replicates). (f) Correlation between quercetin content and MFVD in Tartary buckwheat accessions. Each data point represents one accession. Data are presented as mean ± standard deviation (SD) from three independent biological replicates (n = 3), and significance levels denoted as *P < 0.05, **P < 0.01, and ***P < 0.001.

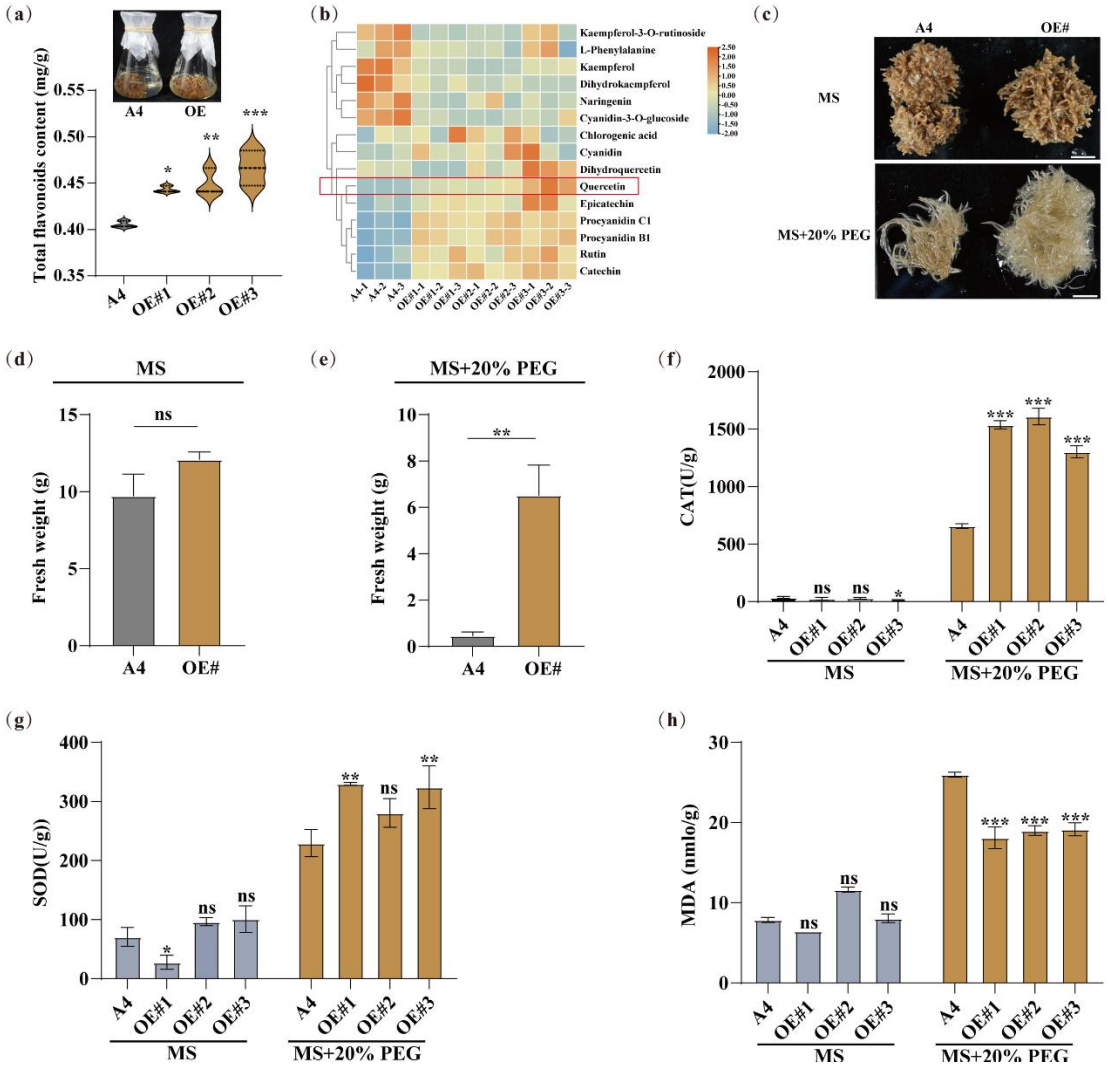

Figure 4 Overexpression of *FtNAC2* in Tartary buckwheat hairy root.

(a) Total flavonoid content in *FtNAC2* overexpressing (OE) hairy roots of Tartary buckwheat. (b) Heatmap representation of differential accumulation of flavonoid compounds in transgenic lines compared to controls. The heatmap depicts quercetin accumulation levels using a continuous color gradient from cool blue (#80B1D3) to warm brown (#EA702D), with increasing color intensity corresponding to higher metabolite concentrations. (c) Hairy root biomass in MS medium (d) without or (e) within 20% PEG-6000. Determination of CAT (f), SOD (g) and MDA (h) in hairy root under natural drought. A4 indicates non-transgenic control hairy roots. For each transgenic line, three independent biological replicates were analyzed to ensure experimental reproducibility. Data are presented as mean ± standard deviation (SD) from three independent biological replicates (n = 3), and significance levels denoted as *P < 0.05, **P < 0.01, and ***P < 0.001.

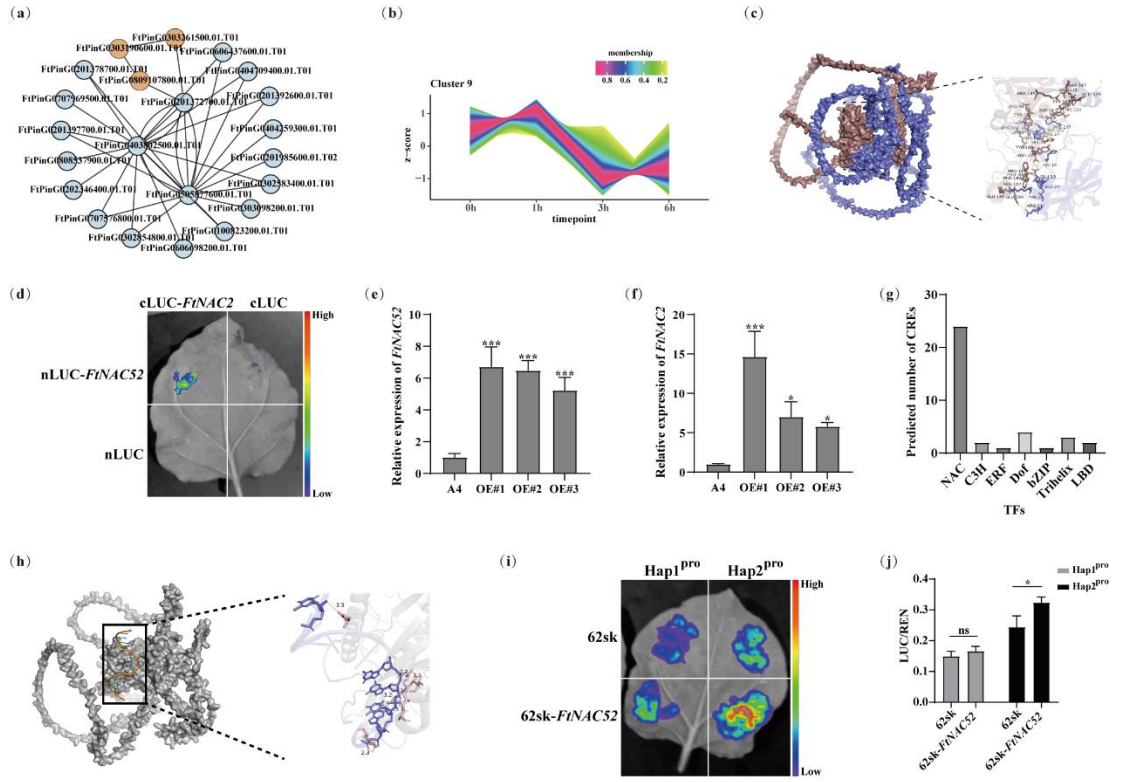

Figure 5 Interaction network prediction and functional analysis of *FtNAC2*.

(a) Protein-protein interaction (PPI) network of *FtNAC2* identified through pull-down assays, showing only interactions associated with *FtNAC2*. (b) Co-cluster pattern of *FtNAC2* and *FtNAC52* within 20% PEG-6000 transcriptome. (c) Predicted three-dimensional interaction interface between FtNAC2 (blue) and FtNAC52 (brown-red) generated by AlphaFold Server, prominently showing only part of the densely binding area due to too much binding sites. (d) Fluorescence complementation detection of the interaction between FtNAC52 and FtNAC2. The relative expression levels of (e) *FtNAC52* and (f) *FtNAC2* in *FtNAC52* overexpression hairy roots in Tartary buckwheat. (g) Statistics of the number of predicted SNPs-related binding element sequences. (h) Predicted molecular interaction between FtNAC2 protein and binding sequence at SNP^{-980}. Structural modeling of FtNAC2 (gray/left and pink/right surfaces) binding to binding sequence (color/left and blue/right surfaces). Yellow dashed lines indicate hydrogen bonds with interatomic distances (Å) labeled. (i-j) Fluorescent quote detection of the activation ability of *FtNAC52* on promoters of different haplotypes. Data are presented as mean ± standard deviation (SD) from three independent biological replicates (n = 3), and significance levels denoted as *P < 0.05.

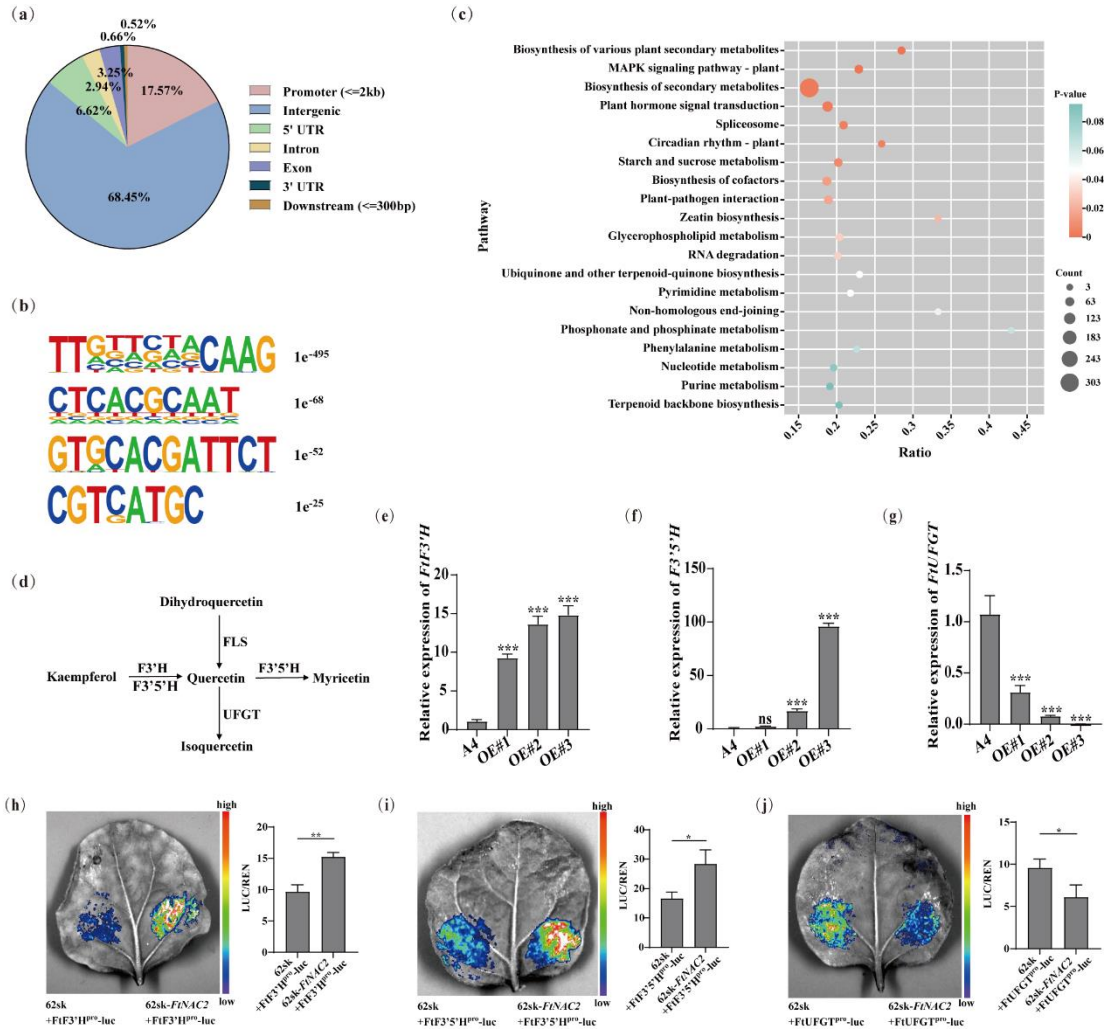

Figure 6 Identification of *FtNAC2* target genes.

(a) Genomic distribution of *FtNAC2* binding peaks identified by DAP-seq, showing the percentage of peaks located in various gene regions. (b) Representative DNA binding motifs significantly enriched in *FtNAC2* binding promoter regions. (c) KEGG pathway enrichment analysis of genes containing *FtNAC2* binding peaks in their promoter regions. (d) Schematic representation of key enzymatic steps in quercetin biosynthesis and modification pathways. (e-g) Expression analysis of quercetin metabolic genes in *FtNAC2* overexpressing hairy roots: relative transcript levels of (e) *FtF3'H (FtPinG0302524300)*, (f) *FtF3'5'H (FtPinG0707657*000), and (g) *FtUFGT* (*FtPinG0707621700*). A4 indicates non-transgenic control hairy roots. (h-j) Regulatory effect of *FtNAC2* on the (h) *FtF3'H*, (i) *FtF3'5'H*, and (j) *FtUFGT* promoters using luciferase signal and LUC/REN ratio. Data are presented as mean ± standard deviation (SD) from three independent biological replicates (n = 3), and significance levels denoted as *P < 0.05, **P < 0.01, and ***P < 0.001.

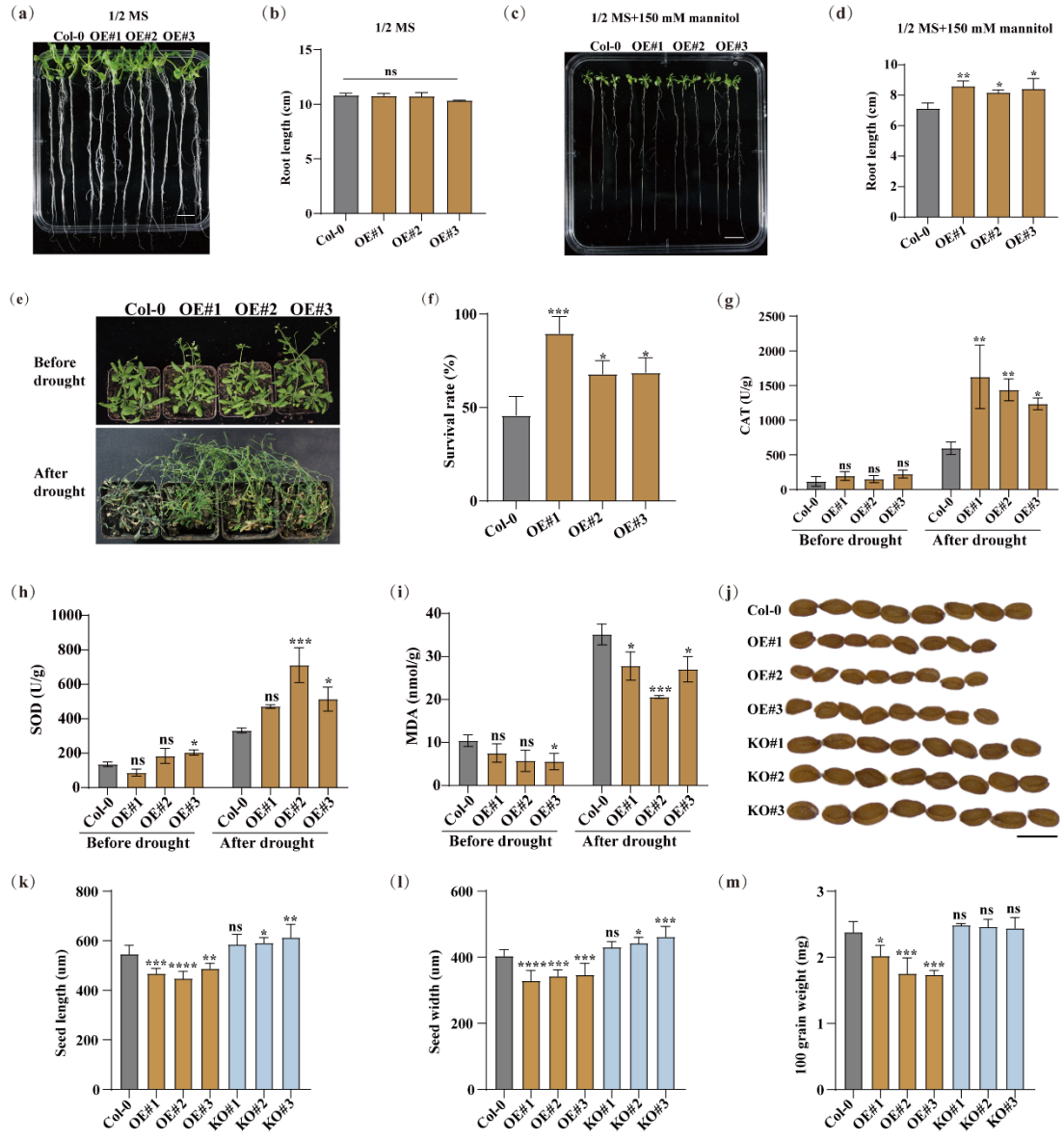

Figure 7 Phenotypic and physiological characterization of *FtNAC2*-related transgenic *Arabidopsis* lines.

(a) Visible phenotypes and (b) survival rates of *Arabidopsis* following natural drought stress. Root length measurements on 1/2 MS medium (c-d) without or (e-f) with 150 mM mannitol osmotic stress (white scale bars = 1 cm). Antioxidant enzyme activities under drought conditions: (g) Catalase (CAT), (h) Superoxide dismutase (SOD), and (i) Malondialdehyde (MDA) levels. Seed morphology analysis: (j) Representative images (black scale bars = 0.5 mm), (k) seed length, (l) seed width, and (m) hundred-seed weight. Col-0 (Columbia wild-type) shown as gray columns, *FtNAC2*-overexpressing (OE#) lines as orange-brown, and knockout (KO#) lines as light blue. Data are presented as mean ± standard deviation (SD) from three independent biological replicates (n = 3), and significance levels denoted as *P < 0.05, **P < 0.01, and ***P < 0.001.

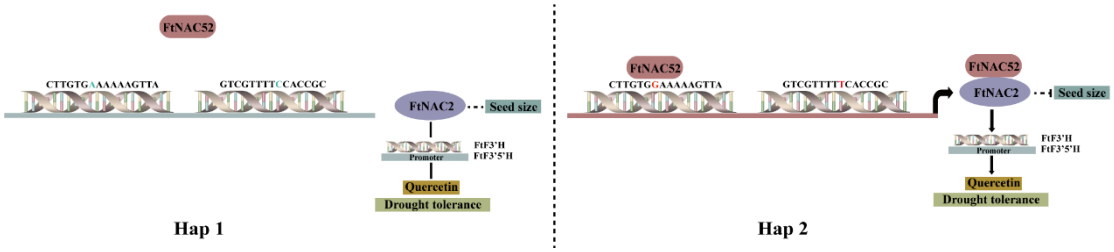

Figure 8. Regulatory model of *FtNAC2*.

Polymorphisms in the *FtNAC2* promoter region regulate gene expression by modulating promoter activity through both direct and indirect mechanisms. Here, we revealed stronger promoter activity in the Hap2 haplotype, and the interacting partner FtNAC52 of FtNAC2 preferentially binds to the Hap2 promoter, collectively enhancing *FtNAC2* expression relative to Hap1. Subsequently, FtNAC2 activates flavonoid hydroxylase genes *FtF3'H* and *FtF3'5'H* through potentially binding to their NAC recognition sequences (NACRS), ultimately increasing quercetin accumulation and conferring improved antioxidant capacity and drought tolerance. The finding in *Arabidopsis* position *FtNAC2* as a multifunctional regulator potentially mediating trade-offs between yield and quality traits in Tartary buckwheat.